Autonomic Neuroscience: Basic and Clinical 156 (2010) 27–35

Contents lists available at ScienceDirect

Autonomic Neuroscience: Basic and Clinical

journal homepage: www.elsevier.com/locate/autneu

Norepinephrine-induced nerve growth factor depletion causes cardiac sympathetic denervation in severe heart failure

Kensuke Kimura *, Hideaki Kanazawa, Masaki Ieda, Haruko Kawaguchi-Manabe, Yoshiko Miyake, Takashi Yagi, Takahide Arai, Motoaki Sano, Keiichi Fukuda

Department of Regenerative Medicine and Advanced Cardiac Therapeutics, Keio University School of Medicine, 35 Shinanomachi, Shinjuku-ku, Tokyo 160-8582, Japan

ARTICLE INFO

Article history:
Received 6 November 2009
Received in revised form 25 February 2010
Accepted 26 February 2010

Keywords:
Sympathetic denervation
Congestive heart failure
Nerve growth factor
Norepinephrine

ABSTRACT

In severe congestive heart failure (CHF), sympathetic overactivity correlates with the exacerbation of cardiac performance. To test the hypothesis that the cardiac sympathetic nerve density dramatically changes with the acceleration of circulating norepinephrine (NE) concentration, we investigated the temporal association of nerve growth factor (NGF) expression in the heart and cardiac sympathetic nerve density during the development of CHF in the continuous NE-infused rats. The animals were analyzed at 0-, 1-, 3-, 7-, 14-, and 28-day after implantation of osmotic pump at a rate of 0.05 mg/kg/hr. The cardiac performance was temporally facilitated in NE-exposed rats at 3-day in accordance with the sympathetic hyper-innervation induced by the augmentation of NGF mRNA expression in the heart. In NE-treated rats, left ventricular end-diastolic pressure was significantly increased after 7-day and marked left ventricular hypertrophy and systemic fluid retention were observed at 28-day. CHF-induced sympathetic overactivity further increased plasma NE concentration in NE-treated rats and finally reached to 16.1 ± 5.6 ng/ml at 28-day (control level was 0.39 ± 0.1 ng/ml, $p<0.01$). In the decompensated CHF rats at 28-day, the NGF mRNA expression was conspicuously reduced concomitant with the obvious nerve fiber loss confirmed by the immunostaining of nerve axonal marker, PGP9.5 and sympathetic neuron marker, tyrosine hydroxylase. This resulted in the attenuated tissue NE contents and the exacerbating cardiac performance. The cardiac sympathetic fiber loss was also confirmed in NE-exposed DBH (dopamine β-hydroxylase)-Cre/Floxed-EGFP (enhanced green fluorescent protein) mice with severe CHF, in which sympathetic nerve could be traced by EGFP. Our results suggest that the cardiac sympathetic nerve density is strictly regulated by the NGF expression in the heart and long-exposure of high plasma NE concentration caused myocardial NGF reduction, following sympathetic fiber loss in severe CHF animals.

1. Introduction

It is well known that plasma norepinephrine (NE) concentration is high in the patients with congestive heart failure (CHF) due to the extreme activation of sympathetic nervous system (SNS), which is progressively augmented corresponding to the severity of CHF (Thomas and Marks, 1978). Moreover, the activation of the cardiac SNS in CHF correlates with the adverse outcome (Cohn et al., 1984). Recent clinical studies have shown that the administration of β-adrenergic receptor blockers improve cardiac performance and reduce cardiac mortality (Packer et al., 1996). NE spillover from sympathetic neurons and the impaired neuronal reuptake have been considered as the major causes of the high plasma concentration in CHF (Hasking et al., 1986; Himura et al., 1993). However, the reduced gene expression of NE synthetic enzyme and NE transporter in the innervated nerves resulting depletion of NE in the failing myocardium cast doubt whether the cardiac sympathetic neurons are still activating in severe CHF (Pool et al., 1967; Eisenhofer et al., 1996). Although the existence of the cardiac-innervated sympathetic neurons which are responsible for synthesizing and secreting NE seems to be of little significance under the circumstance of highly augmented plasma NE level, the innervation anatomy and the source of increased NE overflow remains unexplained so far.

Nerve growth factor (NGF) is a prototypic member of the neurotrophin family, which is critical for the differentiation, maturation, survival, and synaptic activity of the peripheral sympathetic and sensory nervous sytem (Snider, 1994). Expression levels of NGF within innervated tissues roughly correspond to innervations density (Heumann et al., 1984). Some recent studies focused on the decreased myocardial NGF expression in CHF, however the direct evidence of the anatomically "denervated" sympathetic fibers lacked in severe heart failure (Kaye et al., 2000; Qin et al., 2002). We recently reported that the augmentation of NGF expression causes cardiac sympathetic hyperinnervation in the compensated cardiac hypertrophy (Kimura et al., 2007).

* Corresponding author. Tel.: +81 353633874; fax: +81 353633875.
E-mail address: kimuken@cpnet.med.keio.ac.jp (K. Kimura).

1566-0702/$ – see front matter © 2010 Elsevier B.V. All rights reserved.
doi:10.1016/j.autneu.2010.02.005

Given the previous clinical and experimental evidence, we hypothesized that the cardiac sympathetic nerve density dramatically changes with the acceleration of circulating NE concentration and subsequently affects the cardiac performance. To test this hypothesis in vivo, we carried out the present study to examine the temporal association of NGF expression in the heart and cardiac sympathetic nerve density during the development of CHF in the continuous NE-infused rats.

2. Materials and Methods

2.1. Animal experiments

Seven-week old male Wistar rats weighting 240 to 260 g (CLEA Japan,Inc.) were divided into two experimental groups; (1) vehicle-infusion as control groups and (2) NE-infused rats. 0.9% saline with ascorbate (1 mmol/L) vehicle or (-)norepinephrine bitartrate (Sigma Chemical Co.) dissolved in 0.9% saline with ascorbate (1 mmol/L) was administered continuously by subcutaneously implanted osmotic mini pumps (ALZET Osmotic Pumps, model 2004) into the interscapular region. Rats were sedated with ketamine (60 mg/kg) and xylasine (15 mg/kg) given intraperitoneally. NE was infused at a rate of 0.05 mg/kg/hr for maximum 28 days. The animals were killed at 0-, 1-, 3-, 7-, 14-, and 28-day after implantation of osmotic pumps. On the day of the experiment, rats were artificially ventilated under anesthesia with ketamine (60 mg/kg) and xylasine (60 mg/kg) given intraperitoneally. A catheter (HAKKO disposable ELASTER TYPE2, 25G×38 mm) filled with heparin-saline solution, connected to a pressure transducer, was inserted into the thoracic aorta and left ventricle (LV) through the right carotid artery to measure aortic pressure and LV pressure. Mean arterial pressure, LV pressure, LV dp/dt, LV −dp/dt, and heart rate were recorded using a polygraph system (Nihon Kohden). A blood sample (1.5 ml) was then collected from the carotid arterial catheter for measuring plasma NE. The rats were then killed and their hearts, lungs, livers, and left stellate ganglia were removed. Each heart (LV + septum), lung, and liver was weighted. To establish mice that selectively expressed enhanced green fluorescent protein (EGFP) in sympathetic nerves, mice carrying a reporter gene construct chicken β-actin promoter (CAG)-chloramphenicol acetyl transferase (CAT)-EGFP (Kawamoto et al., 2000) were crossed with a mouse line expressing Cre recombinase under the control of the dopamine β-hydroxylase (DBH) promoter (Matsushita et al., 2004). The CAG-CAT EGFP transgenic mouse was a gift from J. Miyazaki (Osaka University, Osaka, Japan). The DBH-Cre recombinase transgenic mouse was provided by K. Kobayashi (Fukushima Medical University, Fukushima, Japan). Five-week-old DBH-Cre/Floxed-EGFP mice were implanted osmotic mini pumps (ALZET Osmotic Pumps, model 2004) into the interscapular region under above-mentioned anesthesia. NE was infused at a rate of 0.05 mg/kg/hr for maximum 28 days. Vehicle-infusion mice were used as controls. The animals were killed at 28-day after implantation of osmotic pumps. All animal experiments approved by the Animal Care and Use Committee of the Keio University.

2.2. Plasma NE measurement

Blood samples were collected in iced heparin-treated tubes containing EDTA-2Na (1 mg/ml) and centrifuged (500×g) at 4 °C for 10 min. Plasma was aliquoted and stored at -20 °C until subsequent assay. NE was assayed by high-performance liquid chromatography (HPLC) with electrochemical detection as described previously (Hjemdahl, 1984).

2.3. Tissue NE measurement

Tissue samples were homogenized within 30 sec in 0.1 N HCl containing 0.1% sodium pyrosulfite (Na2S2O5). After centrifugation (10000 g, 30 min), NE was extracted with alumina and determined by HPLC.

2.4. RNA extraction and poly(A)$^+$RNA Northern Blot Analysis

Total RNA from frozen rat tissue samples (LV + septum) was extracted using TRIzol Reagent (GIBCO BRL), and poly(A)$^+$RNA was isolated. Rat NGF, BNP, and glyceraldehyde-3-phosphate dehydrogenase (GAPDH) cDNA were obtained by RT-PCR from the heart and cloned into the pCRα plasmid. GAPDH cDNA was used as an internal control. Inserts were labeled with [α-^{32}P]dCTP by the random priming technique. A 2.5 μg sample of poly(A)$^+$RNA was run on a 1% MOPS/formaldehyde-agarose gel, and Northern blots were performed as described previously (Sano et al., 2000).

2.5. Immunohistochemical procedures

Sample fixation, embedding, sectioning, and blocking were as described previously (Mabe et al., 2006). To detect nerve fibers in the heart, frozen sections were incubated with double antibodies against protein gene product 9.5 (PGP9.5) (Ultraclone UK, RA95101; 1:2000), growth-associated protein (GAP43) (CHEMICON, AB5220; 1:4000), tyrosine hydroxylase (TH) (CHEMICON, AB152; 1:200), or GFP (Medical&Biological Laboratories, 598; 1:500) and α-Actinin (Sigma, A7811; 1:800). The following secondary antibodies were used: Alexa Fluor 488-conjugated donkky anti-rabbit IgG (Molecular Probes; 1:200), polyclonal swine anti-rabbit TRITC (DAKO; 1:200), Alexa Fluor

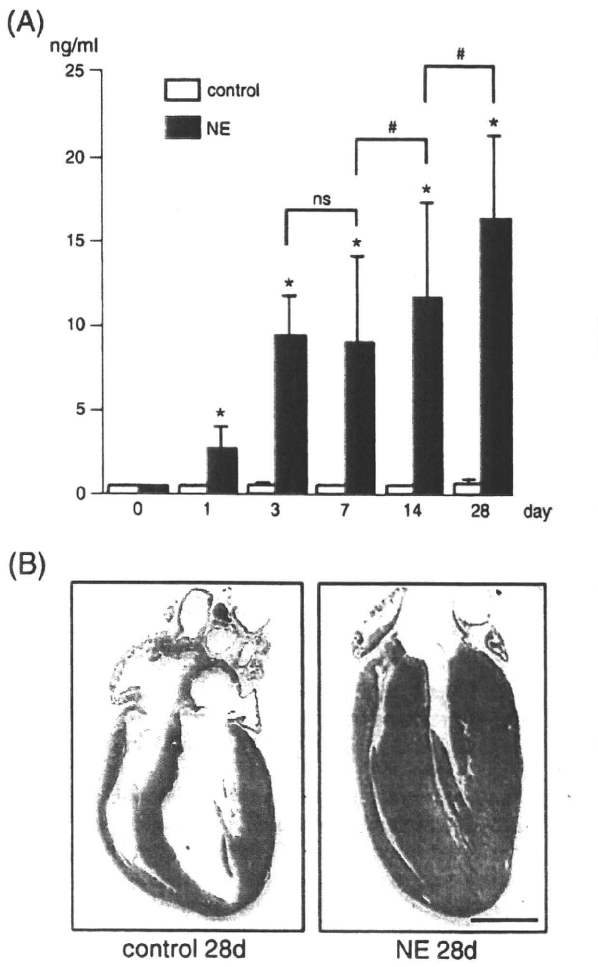

Fig. 1. (A) Plasma concentrations of NE in control and NE-exposed rat. *p<0.01 compared to control at same day, #p<0.01, ns: not significant. (B) Representative section along the long-axis of heart from control and NE-exposed rats at 28-day stained by HE. Note that the LV is markedly thickened and the LV cavity is narrowed. Scale bar indicates 4 mm.

Table 1
Mean wet weight of the tissues in control and NE-treated rats.

	BW (g)	LV + S(mg)	LV + S /body weight (10^{-3})	Lung(mg)	Lung /body weight (10^{-3})	Liver(mg)	Liver /body weight (10^{-3})
Day 0							
Control (n = 7)	248 ± 9	565 ± 49	2.3 ± 0.3	1178 ± 226	4.8 ± 0.4	8320 ± 149	33.5 ± 0.8
NE (n = 8)	259 ± 11	549 ± 25	2.1 ± 0.1	1184 ± 88	4.6 ± 0.7	8470 ± 135	32.7 ± 0.8
Day 1							
Control (n = 8)	245 ± 9	569 ± 17	2.4 ± 0.1	1154 ± 154	4.7 ± 0.7	8286 ± 136	33.8 ± 0.8
NE (n = 14)	254 ± 13	571 ± 38	2.3 ± 0.1	1163 ± 115	4.6 ± 0.9	8433 ± 457	33.2 ± 1.6
Day 3							
Control (n = 8)	267 ± 8	622 ± 41	2.3 ± 0.1	1195 ± 125	4.5 ± 0.5	8619 ± 195	32.3 ± 1.1
NE (n = 15)	258 ± 12	647 ± 64	2.6 ± 0.3	1173 ± 271	4.5 ± 0.5	8590 ± 223	33.3 ± 1.7
Day 7							
Control (n = 8)	273 ± 11	635 ± 17	2.3 ± 0.1	1243 ± 221	4.5 ± 0.6	8872 ± 123	32.5 ± 0.9
NE (n = 12)	267 ± 12	782 ± 72*	2.9 ± 0.3*	1287 ± 169	4.8 ± 0.6	8663 ± 198	32.4 ± 2.2
Day 14							
Control (n = 8)	289 ± 10	638 ± 41	2.2 ± 0.1	1397 ± 153	4.8 ± 0.7	8940 ± 114	30.9 ± 0.4
NE (n = 13)	270 ± 18	862 ± 97*	3.1 ± 0.3*	1375 ± 224	5.1 ± 0.4	8897 ± 251	33.0 ± 1.7
Day 28							
Control (n = 8)	306 ± 13	710 ± 16	2.3 ± 0.1	1473 ± 246	4.8 ± 0.8	9117 ± 108	29.8 ± 0.4
NE (n = 20)	317 ± 21	983 ± 88*	3.2 ± 0.2*	1538 ± 184	4.8 ± 0.9	9430 ± 322	28.8 ± 2.5

*:p 0.01 vs. control.

488-conjugated goat anti-mouse IgG (Molecular Probes; 1:200), and Alexa Fluor 546-conjugated goat anti-mouse IgG (Molecular Probes; 1:200). Apoptosis was measured by using a TUNEL assay kit (Promega). The samples were observed under a Zeiss LSM 510 META confocal microcopy (Germany). Immunostained areas were quantified using NIH image, as described previously (Cao et al., 2000).

2.6. Statistics

Values are presented as means ± SD. The significance of differences among mean values was determined by ANOVA. Statistical comparison of the control group with treated group was carried out using the non-parametric Fisher's multiple comparison tests. The level accepted for significance was $p<0.05$.

3. Results

3.1. Plasma NE concentration

To begin with, to address the characterization of continuous NE infusion model, we measured the plasma NE concentration in the control and NE infusion rats. Plasma NE concentration in NE-treated rats was significantly increased from 1-day after administration compared with control rats. Although the plasma NE level once reached a plateau at around 9 ng/ml between 3-and 7-day, it started to increase after that and finally reached to 16.1 ± 5.6 ng/ml at 28-day (control level was 0.39 ± 0.1 ng/ml, $p<0.01$) (Fig. 1A).

Table 2
Hemodynamic measurements.

	Mean BP (mmHg)	LVEDP (mmHg)	dP/dt (mmHg / sec)	-dP/dt (mmHg / sec)	HR (bpm)
Day 0					
Control (n = 7)	112 ± 4	2.5 ± 0.6	9410 ± 529	6133 ± 643	316 ± 16
NE (n = 8)	103 ± 6	2.9 ± 0.5	9267 ± 416	6318 ± 306	306 ± 24
Day 1					
Control (n = 8)	114 ± 15	3.0 ± 0.6	9333 ± 503	6267 ± 416	316 ± 17
NE (n = 14)	123 ± 9	3.0 ± 0.6	9250 ± 632	6105 ± 469	332 ± 25
Day 3					
Control (n = 8)	118 ± 6	3.1 ± 0.5	9366 ± 423	5917 ± 402	324 ± 30
NE (n = 15)	125 ± 21	5.5 ± 1.4	9467 ± 372	6334 ± 501	339 ± 31
Day 7					
Control (n = 8)	108 ± 16	2.9 ± 0.4	9067 ± 306	5967 ± 153	311 ± 9
NE (n = 12)	127 ± 10	6.7 ± 1.2*	8120 ± 415	5114 ± 458	343 ± 32
Day 14					
Control (n = 8)	103 ± 3	2.9 ± 0.5	9305 ± 436	5907 ± 265	311 ± 9
NE (n = 13)	131 ± 23*	7.9 ± 1.5*	6114 ± 460*	4771 ± 594	349 ± 25
Day 28					
Control (n = 8)	110 ± 4	3.4 ± 0.6	9467 ± 416	6008 ± 296	316 ± 17
NE (n = 20)	143 ± 19*	15 ± 1.9*	5843 ± 476*	3729 ± 419*	360 ± 20*

*:p 0.01 vs. control.

3.2. Appearance and weights

The representative photograph of the longitudinal section of the whole heart in the control and NE-treated rats at 28-day were shown in Fig. 1B. Left ventricular (LV) wall was markedly thickened, and LV cavity was narrowed. Right ventricular free wall was also thickened compared with the control, but less conspicuous than LV. Then, the whole body, LV free wall with septum (S) (LV + S), lung, and liver were separately weighed, and were shown in Table 1. The ratio of LV + S/body weight

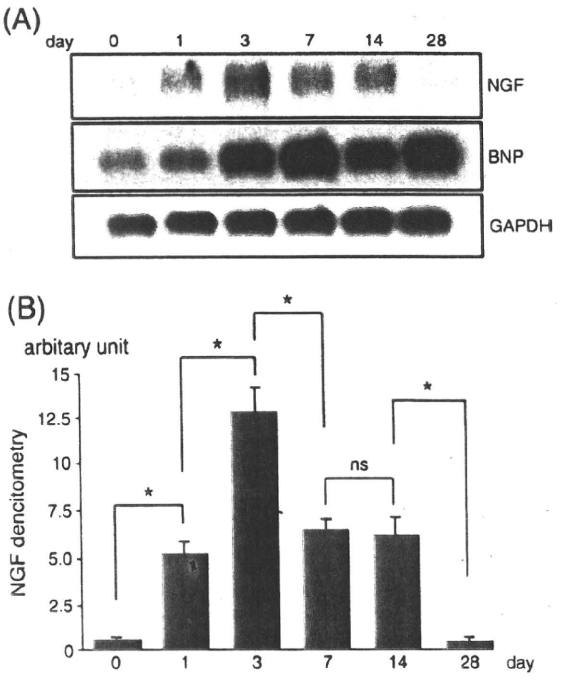

Fig. 2. (A) Northern blot analysis of NGF, BNP, and GAPDH in the left ventricle of NE-exposed rats. (B) Dencitometry analysis of NGF mRNA expression. Northern blot analysis was repeated three times. Expression of NGF mRNA was upregulated at 3-day, subsequently downregulated, and finally almost disappeared at 28-day. *p<0.01, ns: not significant.

(BW) increased from 7-day, and reached by 1.39-fold of the control rats at 28-day. NE-treated rats at-28 day had pleural effusion and ascites. This was the reason why the BW of NE-treated rats at 28- day turned to increase, although those at 14-day decreased compared with control. That was also the cause of unchanged ratio of lung/BW and liver/BW between two groups at 28-day, whereas both lung and liver weight themselves in NE-treated rats were increased. Similarly, the ratio of LV + S/BW in NE-treated rats at 28-day should be much greater than that of controls. These findings indicated that NE treatment for 28 days induced decompensated LV hypertrophy (LVH).

3.3. Hemodynamic measurements

Mean blood pressure of NE-treated rats began to increase at 1-day after NE exposure, significantly increased at 14-day, and reached at 143 ± 19 mmHg (control; 110 ± 4 mmHg) at 28-day (Table 2). LV end-diastolic

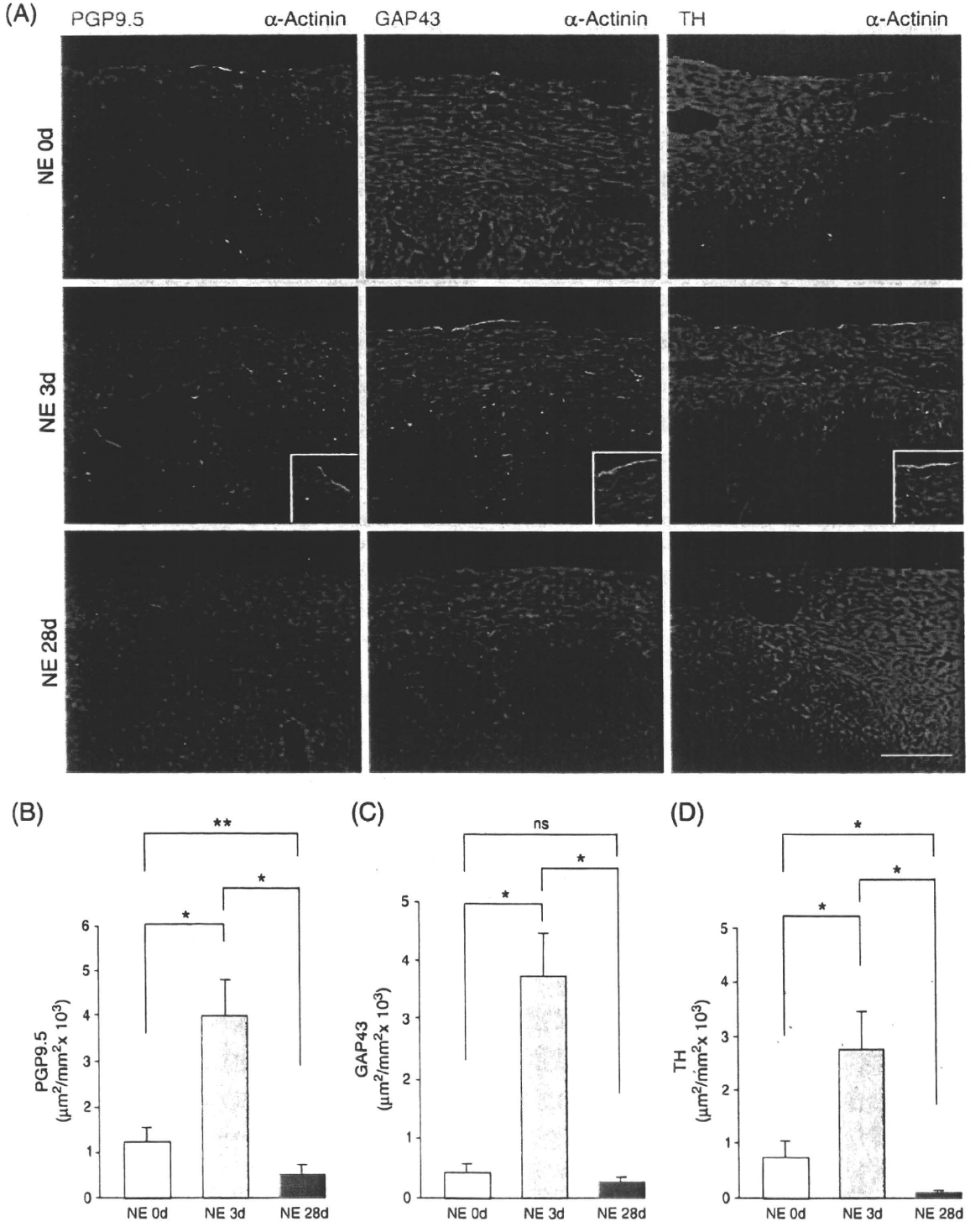

Fig. 3. (A) Double-immunofluorescent staining for PGP9.5, GAP43, and TH with α-Actinin in the LV of 0-, 3-, and 28-day after NE infusion. Insets show high magnification of each sample. (B, C, D) Quantitative analysis of the immunostained area for PGP9.5 (B), GAP43 (C), and TH (D). Scale bar indicates 200 μm. *$p<0.01$, **$p<0.05$, ns: not significant.

pressure (LVEDP) of NE-treated rats started to be raised at 3-day and markedly increased up to 15 ± 1.9 mmHg (control; 3.4 ± 0.6 mmHg) at 28-day. Although it was not significant, it was noteworthy that both dP/dt and |−dP/dt| were temporally elevated in NE-exposed rats at 3-day, whereas these were significantly attenuated at 14-day. Heart rates in NE-infused rats were significantly higher than control at 28-day. These data indicated that NE treatment for 28 days induced heart failure model caused by pressure-overload and/or catecholamine injury.

3.4. NGF and BNP mRNA expression in LV

The performance of NGF mRNA expression in LV of NE-infused rats was immensely unique. In briefly, NGF mRNA was prominently augmented at 3-day after exposure of NE, and after that, it was down-regulated and almost completely disappeared at 28-day. It showed biphasic change through the 28 days. On the other hand, BNP mRNA expression was predictably increased proportionally with the augmentation of LVEDP (Fig. 2 and Table 2).

3.5. Immunohistochemistory for nerve density in heart section

Levels of NGF expression within innervated tissue roughly correspond to innervation density. Thus, we performed an immunohistochemical staining of protein gene product 9.5 (PGP9.5), growth associated protein 43 (GAP43) and tyrosine hydroxylase (TH) to evaluate the nerve density. The PGP9 5 is specifically expressed in nerve fiber axon. GAP43 is a protein that was expressed when the nerve terminal develops. TH is an enzyme that catalyzes the conversion of L-tyrosine to L-DOPA and is a rate-determining enzyme for catecholamine synthesis. For this reason, it is used as a marker of sympathetic nerves. Interestingly, there was a remarkable increase in the expression of PGP9.5, GAP43, and TH in the LV at 3-day after administration of NE. Newly developed nerves were prominent at the

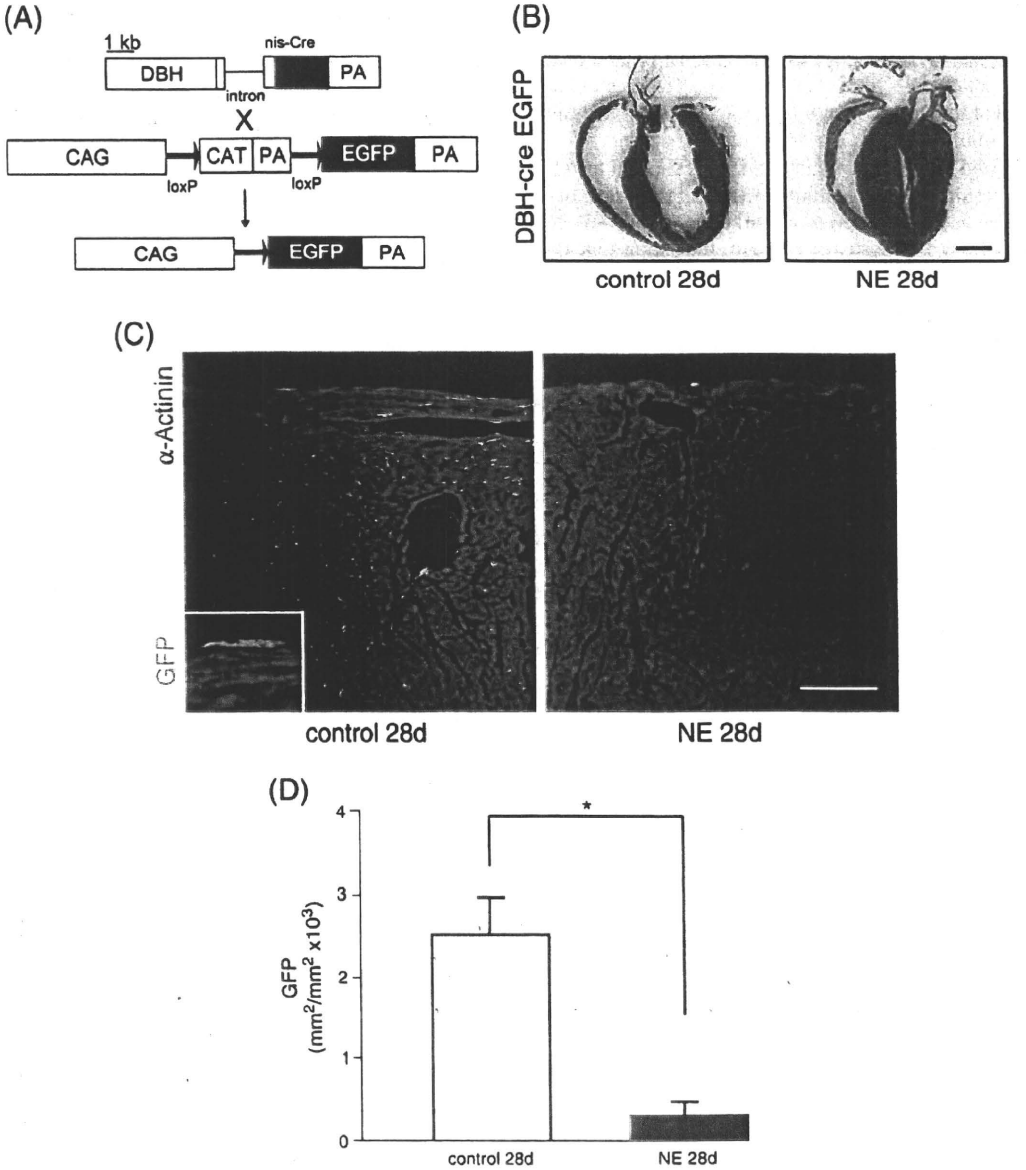

Fig. 4. (A) Dopamine β-hydroxylase (DBH)-Cre transgenic mice were crossed with CAG-CAT-EGFP mice. In the double-transgenic mice ($Cre^+/EGFP^+$), Cre-loxP recombination deletes the CAT gene cassette, leading to the expression of EGFP in sympathetic neurons. (B) Representative section of heart along the long axis from control and NE-infused mice (28-day) stained by HE. Scale bar indicates 2 mm. (C) Double- immunofluorescent staining for GFP and α-Actinin in the LV of control and NE-infused mice at 28-day. Inset shows high magnification. Scale bar indicates 200 μm. (D) Quantitative analysis of the immunostained area for GFP in the LV of control and NE-infused mice. *$p<0.01$.

epicardial layer or the perivascular area, indicated sympathetic neurons (Fig. 3A). The quantitative analysis revealed that PGP9.5, GAP43, and TH increased 3.2-fold, 9.1-fold, and 3.8-fold respectively, in LV at 3-day after NE administration compared with 0-day. (Fig. 3B, C, D). In contrast, not only growth cone marker GAP43 -immunostained neurons, but also nerve fiber marker PGP9.5-immunostained neurons were conspicuously down-regulated in decompensated hypertrophic LV at 28-day (Fig. 3A). The quantitative analysis revealed that the immunostained area of PGP9.5 and TH at 28-day decreased by 88% and 95%, respectively of that at 3-day and also decreased by 58% and 88%, respectively of that at 0 day. The immunostained area of GAP43 at 28-day down-regulated by 92% of that at 3- day, but there was no significant difference between 0-day and 28-day (Fig. 3B, C). These data indicated that sympathetic nerve density in LV was directly correlated with the NGF expression.

3.6. Cardiac sympathetic nerve density in NE-infused mice using the Cre-LoxP system

To confirm whether cardiac sympathetic nerve density is truly attenuated by long-time exposure of NE, we next prepared double-transgenic conditional knockouts by crossing mice carrying a floxed CAT- CAG- EGFP allele with mice that expressed Cre recombinase under the control of the DBH promoter (Fig. 4A), and subjected them to continuous NE infusion to induce heart failure. The adrenergic cells of brain, adrenal, and stellate ganglia in these mice showed a strong GFP signal (data not shown). Longitudinal sections of the whole heart in NE-infused mice at 28-day showed a marked LVH (Fig. 4B). NE-treated mice at 28-day had systemic effusion, indicating that they were in the decompensated stage of heart failure. Immunostaining revealed that GFP signal were markedly decreased in the LV in NE-injected mice at 28-day (Fig. 4C), with the positively stained areas for GFP in the LV following NE-infusion decreased by 87% compared to controls (Fig. 4D). These data confirmed that long-term NE administration causes the anatomical cardiac sympathetic denervation concomitant with severe heart failure.

3.7. Tissue NE content in LV

The NE that is present in the heart is located in the sympathetic nerve fibers rather than in the myocardium per se. To investigate the alteration of sympathetic nerve density could correspond to the sympathetic terminal NE stores, we measured the NE content of the LV tissue in the control and NE-exposed rats. The NE content at 3-day in the LV of the NE-exposed rats tremendously increased 2.1-fold compared with the control at 3- day, sequentially down-regulated, and markedly decreased at 28-day (Fig. 5). These data indicated that the NGF-dependent sympathetic innervation greatly influenced the patterning of the tissue NE content in the LV and LV performance estimated by dP/dt and -dP/dt (Fig. 5 and Table 2).

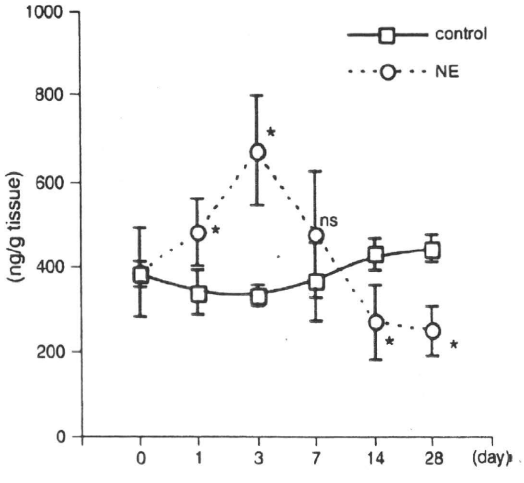

Fig. 5. Tissue NE concentrations in the LV of control and NE-infused rats. *$p<0.01$ compared to control at same day. ns: not significant between control and NE-infused at 7-day.

3.8. Analysis of neuronal cell bodies in stellate ganglion

To investigate whether NE-toxicity directly affects the apoptosis of sympathetic nerve cell body in stellate ganglion, we examine TUNEL assay and count the number of neuronal cell bodies at 0-, 3-, and 28-day in NE-infused rats. The small number of TUNEL positive cells was only observed in the interstitial cells, but not in the neuronal cell bodies at either 0-, 3-, or 28-day (Fig. 6A). Moreover, the number of neuronal cell bodies in stellate ganglion was not significantly different among 0-, 3-, and 28-day (Fig. 6B).

4. Discussion

4.1. Character of NE-infusion model

Continuous NE administration by osmotic pump effectively maintained the high plasma NE concentration throughout 28 days in rats. The level of the concentration reached to a plateau at 3-day after exposure, maintaining the level until 7-day, however it seemed to exceed the estimated value at 28-day. It is generally known that in patients with advanced heart failure, the circulating NE concentration is higher than the level found in normal subjects (Meredith et al., 1993). In our model at 28-day, the higher plasma NE level was presumably modified by heart failure, that is to say, NE induced NE release. As evidenced by the retention of pleural effusion and ascites accompanied with weight gain and the prominent increase of LVEDP, the NE- infused rats at 28-day presented decompensated phase of heart failure. The mean blood pressure of NE-infused rats at 28 day was significantly increased, however compared with the other high blood pressure model, e.g. transaortic constriction mouse or Dahl salt sensitive rat, the level was not enough to produce pressure overload induced heart failure (Sheikh et al., 2008; Miyachi et al., 2009). For the reason of these, we estimated the main etiology of cardiomyopathy in this model as a result of NE induced cardiac injury with hypertrophy directly derived from NE.

4.2. Sympathetic hyper-innervation phase towards hypertrophy

The cardiac performance of NE-exposed rats temporally accelerated at 3 day. Around this phase, cardiac muscles were started to be driven by the increasing circulatory NE via β1 adrenergic receptors. Moreover, at that time, we confirmed that NE content in the sympathetic nerve terminal was also upregulated, reasonably accompanied by sympathetic hyperinnervation. Locally released NE from hyperinervated nerve terminals was presumably more effective in controlling cardiac performance than circulatory NE (Chang et al., 1991). Needless to say, NE itself is a strong cardiac hypertrophic factor and it also derives other hypertorphic factors, e.g. endothelin-1(ET-1), angiotensin II, leukemia inhibitory factor (LIF), from cardiomyocytes (Okada et al., 1995; Baker et al., 1990; Wang et al., 2001). Among these factors, ET-1 has been proven as a factor which can induce NGF expression in cardiomyocytes via ET-A receptor/Giβγ pathway (Ieda et al., 2004). In this study, we observed the augmented NGF expression in the LV of NE-infused rat at 3-day. Although we did not examine the expression of ET-1 in this study, we speculated that the augmented expression of NGF was presumably elicited by ET-1. This speculation is strongly supported by the study of Kaddoura et al. They reported that ventricular expression of ET-1 mRNA is elevated in the first 3 days and falls after that in NE-infused rat (Kaddoura et al., 1996). Moreover, we recently reported that the augmented NGF mRNA expression concomitant with upregulated ET-1 mRNA causes cardiac sympathetic hyperinnervation in pressure-

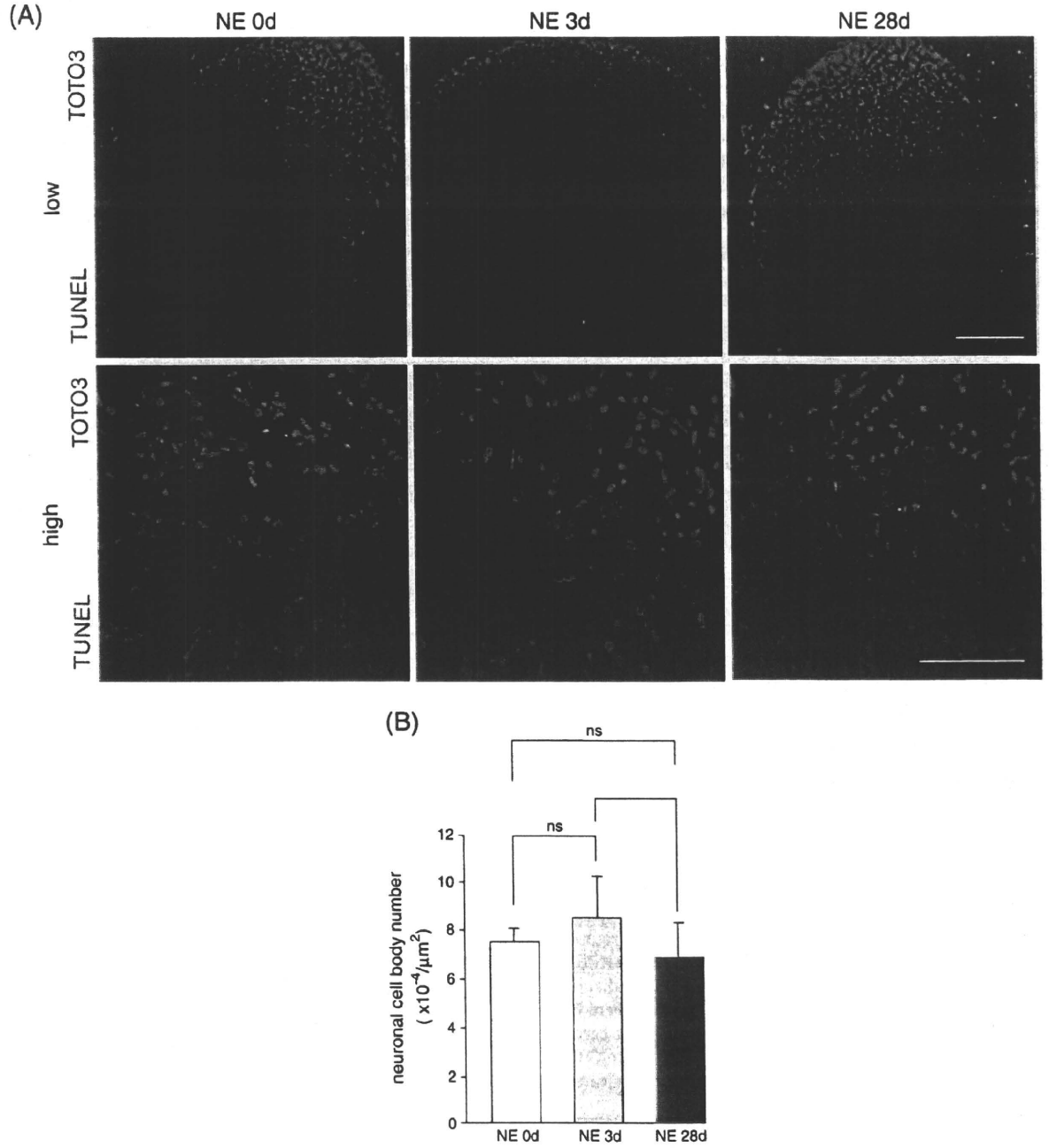

Fig. 6. (A) TUNEL staining in left stellate ganglion of 0-, 3-, and 28-day after NE infusion. Upper panels show low magnification (scale bar indicates 50 μm) and lower panels show high magnification (scale bar indicates 100 μm). (B) Quantitative analysis of the neuronal cell body number in the stellate ganglion in 0-, 3-, and 28-day (n = 5, respectively) of NE-infused mice. ns: not significant.

overload induced cardiac hypertrophy (Kimura et al., 2007). It is noteworthy that the number of neuronal cell bodies in stellate ganglion was not significantly increased at 3-day after NE infusion, indicating the sympathetic fibers were sprouted from the peripheral knots by the augmented NGF expression.

Taken together, our data indicated that the cardiac hyperinnervation induced by the enhanced NGF expression influenced the facilitation of cardiac performance in the early period of NE-infused animals.

4.3. Sympathetic denervation phase during heart failure

In our study, the NGF mRNA expression was enormously down-regulated concomitant with the high plasma concentration in NE-infused rats at 28-day. This resulted in the cardiac sympathetic denervation and attenuated tissue NE contents. We also clearly showed that cardiac sympathetic fibers were markedly reduced in NE-induced heart failure mice, in which sympathetic nerves could be traced by EGFP. Furthermore, we showed no clear evidence of that NE-toxicity directly affects apoptosis of sympathetic neurons in stellate ganglion. These results suggest that long- exposure of NE causes the NGF depletion in the heart, which secondary affects the retreating of peripheral sympathetic fibers from the heart. Our results are strongly supported by the following two studies. Qin et al. reported that NE-mediated reduction of NGF and its neurotrophic receptor tyrosine kinase A (TrkA) involve in the decrease of sympathetic neurotransmitter in heart failure in vivo (Qin et al., 2002). Kaye et al. reported NE

exposure reduced NGF expression in isolated cardiomyocytes (Kaye et al., 2000). Although direct correlation between NGF level and sympathetic nerve density has not been examined in these papers, they showed that TrkA expression and tyrosine hydroxylase profile were decreased in CHF and NE-infused animals, indicating sympathetic denervation. The mechanism of NE induced NGF downregulation in vivo still remains unexplained. In vitro study, Kaye showed the reduced NGF expression is achieved by 10 μmol NE via α-adrenergic receptor-coupled protein kinase C signal pathway (Kaye et al., 2000). This NE concentration in the medium is almost 100 times higher than the plasma concentration of our NE-infusion model at 28-day, whereas we presume that the myocardial injury dependent on NE-exposed time and dose might affect the several gene expressions which regulate NGF production from cardiomyocytes in vivo. Recently, Rana et al showed that mechanical stretch and α-1-adrenergic stimulation attenuate the NGF expression via the calcineurin-NFAT signaling pathway in cultured neonatal cardiomyocyte (Rana et al., 2009). The renin-angiotensin-aldosterone system is also activated in heart failure, however, little is known as to how it affects the NGF reduction in severe heart failure. Additional studies are needed to investigate the precise mechanism in vivo.

4.4. Significance from clinical viewpoint

Many studies demonstrated a high plasma NE concentration concomitant with a depressed MIBG reuptake in CHF, and this phenomenon has been explained as sympathetic denervation (Henderson et al., 1988). A general definition of denervation seems to include two meanings. One is functional denervation. As we know, NE uptake activity in sympathetic nerve ends is reduced in CHF, and this is considered as a general mechanism in attenuated MIBG reuptake. Elevated NE level is attributed in the development of cardiac sympathetic nerve terminal abnormalities in CHF (Bohm et al., 1995). And we have recently reported that pressure overload induces the rejuvenation of cardiac sympathetic nerve and LIF and cardiotrophin-1, derived from failing heart, give rise to the cholinergic transdifferentiation in cardiac sympathetic nerve via gp130 signaling pathway, causing the functional sympathetic denervation in CHF (Kimura et al., 2007, Kanazawa et al., 2010).

Second is anatomical denervation, which is more rigorous definition of the word. In this study, we demonstrated that long-exposure of high plasma concentration of NE caused myocardial NGF reduction, following peripheral sympathetic fiber loss in severe CHF animals. Moreover, nerve loss and reduced NE content in cardiac tissue obviously indicated that plasma NE elevation in severe CHF is derived from peripheral organs, but not a spillover from the cardiac sympathetic nerve ends.

We speculated that functional sympathetic denervation precedes anatomical denervation and the latter could be observed in the advanced stage of heart failure accompanied with long-exposure of high plasma NE. Because our previous study showed that the augmentation of LIF and cardiotrophin-1 in failing heart rather than NGF reduction affects the cardiac sympathetic function via cholinergic transdifferentiation in heart failure models, such as transaortic constriction mice and Dahl salt sensitive rats (Kanazawa et al., 2010). In these conventional models, duration and level of the high plasma NE concentration might be insufficient to affect the NGF reduction.

In human severe CHF, there are huge evidence that protective therapy against catecholamine-toxicity improve cardiac function and prognosis. We are interested in how β-blocker therapy may affect these processes in sympathetic nerve loss.

Furthermore, as we showed, the cardiac NGF depletion did not result in the neuronal cell death, which occurred to us that NGF supplement therapy might be effective for the improvement in cardiac function in severe CHF (Kreusser et al., 2006). We are also interested in the influence of high plasma NE concentration on parasympathetic neurons. Further, it has been known that sympathetic denervation is also observed in diabetic heart. Although it could be explained by depletion of the neurotrophic factors, little is known about the precise mechanism in diabetic neuropathy. Thus, further studies will be required to investigate the peculiar mechanism of cardiac denervation in each disease.

Acknowledgements

This study was supported in part by the research grants (10B-1) of "Nervous and Mental Disorders from the Ministry of Health and Welfare" and research grants from the Ministry of Education, Science and Culture, Japan, and Health Science Research Grants for Advanced Medical Technology from the Ministry of Welfare, Japan.

References

Baker, K.M., Chernin, M.I., Wixson, S.K., Aceto, J.F., 1990. Renin-angiotensin system involvement in pressure-overload cardiac hypertrophy in rats. Am. J. Physiol. 259, H324–H332.

Bohm, M., La Rosee, K., Schwinger, R.H., Erdmann, E., 1995. Evidence for reduction of norepinephrine uptake sites in the failing human heart. J. Am. Coll. Cardiol. 25, 146–153.

Cao, J.M., Fishbein, M.C., Han, J.B., Lai, W.W., Lai, A.C., Wu, T.J., Czer, L., Wolf, P.L., Denton, T.A., Shintaku, I.P., Chen, P.S., Chen, L.S., 2000. Relationship between regional cardiac hyperinnervation and ventricular arrhythmia. Circ. 101, 1960–1969.

Chang, P.C., Kriek, E., van der Krogt, J.A., van Brummelen, P., 1991. Does regional norepinephrine spillover represent local sympathetic activity? Hypertens. 18, 56–66.

Cohn, J.N., Levine, T.B., Olivari, M.T., Garberg, V., Lura, D., Francis, G.S., Simon, A.B., Rector, T., 1984. Plasma norepinephrine as a guide to prognosis in patients with chronic congestive heart failure. N Engl J. Med. 311, 819–823.

Eisenhofer, G., Friberg, P., Rundqvist, B., Quyyumi, A., Lambert, G., Kaye, D., Kopin, I., Goldstein, D., Esler, M., 1996. Cardiac sympathetic nerve function in congestive heart failure. Circ. 93, 1667–1676.

Hasking, G.J., Esler, M.D., Jennings, G.L., Burton, D., Korner, P.I., 1986. Norepinephrine spillover to plasma in patients with congestive heart failure: evidence of increased overall and cardiorenal sympathetic nervous activity. Circ. 73, 615–621.

Henderson, E.B., Kahn, J.K., Corbett, J.R., Jansen, D.E., Pippin, J.J., Kulkarni, P., Ugolini, V., Akers, M.S., Hansen, C., Buja, L.M.., 1988. Abnormal I-123 metaiodo-benzylguanidine myocardial washout and distribution may reflect myocardial adrenergic derangement in patients with congestive cardiomyopathy. Circ. 78, 1192–1199.

Heumann, R., Korsching, S., Scott, J., Thoenen, H., 1984. Relationship between levels of nerve growth factor (NGF) and its messenger RNA in sympathetic ganglia and peripheral target tissues. EMBO J. 3, 3183–3189.

Himura, Y., Felten, S.Y., Kashiki, M., Lewandowski, T.J., Delehanty, J.M., Liang, C.S., 1993. Cardiac noradrenergic nerve terminal abnormalities in dogs with experimental congestive heart failure. Circ. 88, 1299–1309.

Hjemdahl, P., 1984. Catecholamine measurements by highperformance liquid chromatography. Am. J. Physisl. 247, E13–E20.

Ieda, M., Fukuda, K., Hisaka, Y., Kimura, K., Kawaguchi, H., Fujita, J., Shimoda, K., Takeshita, E., Okano, H., Kurihara, Y., Kurihara, H., Ishida, J., Fukamizu, A., Federoff, H.J., Ogawa, S., 2004. Endothelin-1 regulates cardiac sympathetic innervations in the rodent heart by controlling nerve growth factor expression. J. Clin. Investig. 113, 876–884.

Kaddoura, S., Firth, J.D., Boheler, K.R., Sugden, P.H., Poole-Wilson, P.A., 1996. Endothelin-1 is involved in norepinephrine-induced ventricular hypertrophy in vivo. Circ. 93, 2068–2079.

Kanazawa, H., Ieda, M., Kimura, K., Arai, T., Kawaguchi-Manabe, H., Endo, J., Kawakami, T., Kimura, T., Monkawa, T., Hayashi, M., Iwanami, A., Shimoda, K., Okano, H., Okada, Y., Ishibashi-Ueda, H., Ogawa, S., Fukuda, K., 2010. Heart failure causes cholinergic transdifferentiation of cardiac sympathetic nerves via gp130-mediated cytokines. J. Clin. Investig. 120, 408–421.

Kawamoto, S., Niwa, H., Tashiro, F., Sano, S., Kondoh, G., Takeda, J., Tabayashi, K., Miyazaki, J., 2000. A novel reporter mouse strain that expresses enhanced green fluorescent protein upon Cre-mediated recombination. FEBS Lett. 470, 263–268.

Kaye, D.M., Vaddadi, G., Gruskin, S.L., Du, X.J., Esler, M.D., 2000. Reduced myocardial nerve growth factor expression in human and experimental heart failure. Circ. Res. 86, 80–84.

Kimura, K., Ieda, M., Kanazawa, H., Yagi, T.K.T., Tsunoda, M.N.S., Kurosawa, H., Yoshimi, K., Mochizuki, H., Yamazaki, K., Okada, Y., Ogawa, S., Fukuda, K., 2007. Cardiac sympathetic rejuvenation: a link between nerve function and cardiac hypertrophy. Circ. Res. 100, 1755–1764.

Kreusser, M.M., Haass, M., Buss, S.J., Hardt, S.E., Gerber, S.H., Kinscherf, R.K., Katus, H.A., Backs, J., 2006. Injection of nerve growth factor into stellate ganglia improves norepinephrine reuptake into failing hearts. Hypertens. 47, 209–215.

Mabe, A.M., Hoard, J.L., Duffourc, M.M., Hoover, D.B., 2006. Localization of cholinergic innervation and neurturin receptors in adult mouse heart and expression of the neurturin gene. Cell Tissue Res. 326, 57–67.

Matsushita, N., Kobayashi, K., Miyazaki, J., Kobayashi, K., 2004. Fate of transient catecholaminergic cell types revealed by site-specific recombination in transgenic mice. J. Neurosci. Res. 78, 7–15.

Meredith, I., Eisenhofer, G., Lambert, G., Dewar, E., Jennings, G., Esler, M., 1993. Cardiac sympathetic nervous activity in congestive heart failure: evidence for increased neuronal norepinephrine release and preserved neuronal uptake. Circ. 88, 136–145.
Miyachi, M., Yazawa, H., Furukawa, M., Tsuboi, K., Ohtake, M., Nishizawa, T., Hashimoto, K., Yokoi, T., Kojima, T., Murate, T., Yokota, M., Murohara, T., Koike, Y., Nagata, K., 2009. Exercise training alters left ventricular geometry and attenuates heart failure in dahl salt-sensitive hypertensive rats. Hypertens. 53, 701–707.
Okada, M., Yamashita, C., Okada, M., Okada, K., 1995. Role of endothelin-1 in beagles with dehydromonocrotaline-induced pulmonary hypertension. Circ. 92, 114–119.
Packer, M., Bristow, M.R., Cohn, J.N., Colucci, W.S., Fowler, M.B., Gilbert, E.M., Shusterman, N.H., 1996. The effect of carvedilol on morbidity and mortality in patients with chronic heart failure. N Engl J. Med. 334, 1349–1355.
Pool, P.E., Covell, J.W., Levitt, M., Gigg, J., Braunwald, E., 1967. Reduction of cardiac tyrosine hydroxylase activity in experimental congestive heart failure: its role in the depletion of cardiac norepinephrine stores. Circ. Res. 20, 349–353.
Qin, F., Vulapalli, R.S., Stevens, S.Y., Liang, C.S., 2002. Loss of cardiac sympathetic neurotransmitters in heart failure and NE infusion is associated with reduced NGF. Am. J. Physiol. 282, H363–H371.
Rana, O.R., Saygili, E., Meyer, C., Gemein, C., Krüttgen, A., Andrzejewski, M.G., Ludwig, A., Schotten, U., Schwinger, R.H.G., Weber, C., Weis, J., Mischke, K., Rassaf, T., Kelm, M., Schauerte, P., 2009. Regulation of nerve growth factor in the heart: The role of the calcineurin-NFAT pathway. J. Mol. Cell. Cardiol. 46, 568–578.
Sano, M., Fukuda, K., Kodama, H., Pan, J., Saito, M., Matsuzaki, J., Takahashi, T., Makino, S., Kato, T., Ogawa, S., 2000. Interleukin-6 family of cytokines mediate angiotensin II-induced cardiac hypertrophy in rodent cardiomyocytes. J. Biol. Chem. 275, 29717–29723.
Sheikh, F., Raskin, A., Chu, P.H., Lange, S., Domenighetti, A.A., Zheng, M., Liang, X., Zhang, T., Yajima, T., Gu, Y., Dalton, N.D., Mahata, S.K., Dorn II, G.W., Heller-Brown, J., Peterson, K.L., Omens, J.H., McCulloch, A.D., Chen, J., 2008. An FHL1-containing complex within the cardiomyocyte sarcomere mediates hypertrophic biomechanical stress responses in mice. J. Clin. Investig. 118, 3870–3880.
Snider, W.D., 1994. Functions of the neurotrophins during nervous system development: what the knockouts are teaching us. Cell 77, 627–638.
Thomas, J.A., Marks, B.H., 1978. Plasma norepinephrine in congestive heart failure. Am. J. Cardiol. 41, 233–243.
Wang, F., Seta, Y., Baumgarten, G., Engel, D.J., Sivasubramanian, N., Mann, D.L., 2001. Functional significance of hemodynamic overload-induced expression of leukemia-inhibitory factor in the adult mammalian heart. Circ. 103, 1296–1302.

Circulation Journal
Official Journal of the Japanese Circulation Society
http://www.j-circ.or.jp

REVIEW

Cardioprotection by Hormetic Responses to Aldehyde

Motoaki Sano, MD, PhD

Everyone encounters various stressors (causes of stress), such as psychological pressure, mental fluctuations, and physical burdens, in their everyday life. It is well accepted that the highest levels of perceived stress correlate with early onset of cardiovascular disease. Conversely, appropriate (mild to moderate) stressors, such as physical activity, have been shown to promote health. This bidirectional dose–response relationship of treatments that are beneficial at low levels but noxious at higher levels is referred to as "hormesis". In the fields of toxicology, pharmacology, radiation biology, and medicine, the significance of the biological effects of low-level exposure to various agents has attracted considerable attention. It is very important to understand how biological systems respond to low levels of stress and their implications within society. Aldehydes, the major endproducts of lipid peroxidation, have been implicated in the pathogenesis of oxidative stress-associated diseases. In addition to the pathogenic effect associated with oxidative stress, sublethal levels of aldehydes interact with signaling systems to upregulate the expression of genes to counteract the stressor challenge and to re-establish homeostasis. The present review article discusses current discoveries regarding the hormetic response to aldehyde and its clinical significance in cardioprotection. (*Circ J* 2010; **74:** 1787–1793)

Key Words: Antioxidants; Metabolism; Myocardial infarction; Oxidative stress; Stress

We all encounter various stressors (causes of stress), such as psychological pressure, mental fluctuations, and physical burdens, in everyday life. It is well accepted that the highest levels of perceived stress correlate with the early onset of cardiovascular disease. Chronic stress facilitates plaque formation in the coronary arteries; superimposed acute stress often triggers plaque rapture and thrombosis, leading to myocardial infarction, a major cause of sudden death.

Recent studies have demonstrated that stress affects health by modulating the rate of cellular aging. Telomeres are DNA–protein complexes that cap chromosomal ends and promote chromosomal stability. Telomeres become shorter with every replication of the cell and telomerase status and telomere length are well-established indices of cellular aging.[1] For example, the telomere length in peripheral blood mononuclear cells (PBMC) from healthy premenopausal mothers of chronically ill children is significantly shorter than that in the PBMC of age-matched mothers of healthy children.[2]

Conversely, appropriate (mild to moderate) stressors have been shown to promote health. For example, there is documented evidence of the significant health benefits of physical activity. Physical activity is known to decrease the risk of premature mortality in general and the risk of coronary artery disease, hypertension, colon cancer, and diabetes mellitus in particular. Beyond the cardiovascular health benefits of physical exercise, the positive effects of exercise on mental health and cognitive function have also come to public attention. There is a positive correlation between aerobic capacity and brain tissue density in middle-aged men and women, with physical exercise seemingly slowing brain aging.[3] Such an effect in the human brain has major implications in terms of delaying the onset of conditions such as dementia and Alzheimer's disease.

Recent studies have shown that exercise prevents the destruction of telomeres; however, the relationship between the level of physical activity and telomere length seems to be bidirectional. Moderate exercise results in significantly longer PBMC telomere length compared with very low exercise levels, but these benefits are not necessarily seen with higher levels of exercise.[4]

These bidirectional dose–response relationships of treatments that are beneficial at low levels but noxious at higher levels are referred to as "hormesis".[5] In the fields of toxicology, pharmacology, radiation biology, and medicine, the significance of the biological effects of low-level exposure to various agents has attracted considerable attention. Stress response hormesis refers to the induction, by stressors, of an adaptive response that results in a general increase in stress resistance.[6] It is very important to understand how biological systems respond to low levels of stress and the implications within society. The present review article discusses current discoveries regarding the hormetic response to aldehyde and its clinical significance in cardioprotection.

Received July 22, 2010; accepted July 22, 2010; released online August 12, 2010
Department of Cardiology, Keio University School of Medicine, Tokyo, Japan
Mailing address: Motoaki Sano, MD, PhD, Department of Cardiology, Keio University School of Medicine, 35 Shinanomachi, Shinjuku-ku, Tokyo 160-8582, Japan. E-mail: msano@sc.itc.keio.ac.jp
ISSN-1346-9843 doi:10.1253/circj.CJ-10-0716

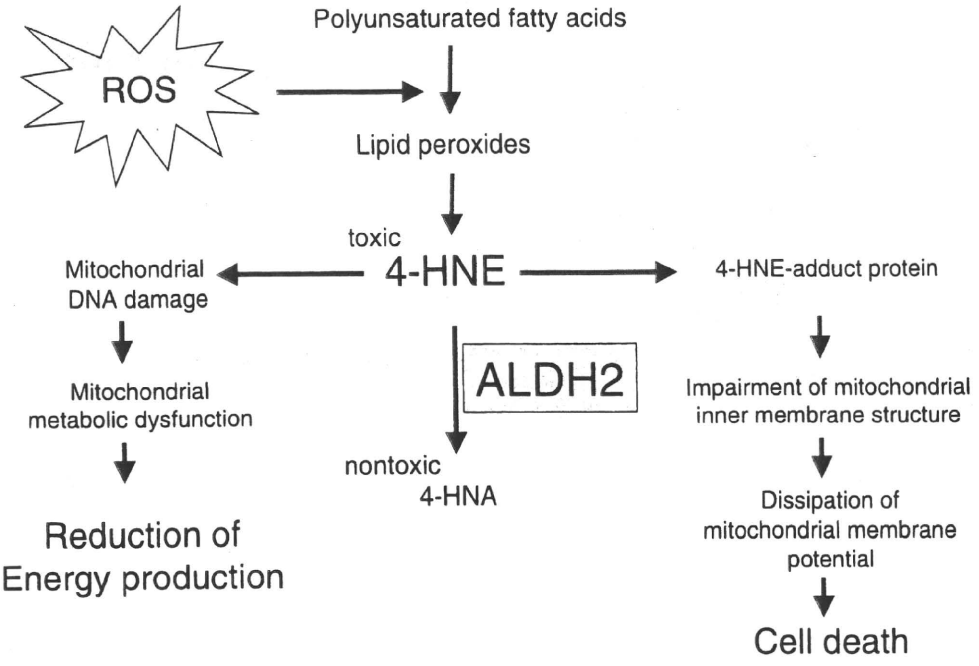

Figure 1. Much of the oxidative stress-associated damage can be attributed to aldehydes. ROS, reactive oxygen species; 4-HNE, 4-hydroxy-2-nonenal; ALDH2, aldehyde dehydrogenase 2.

What Is Aldehyde?

Acetoaldehydes are produced following alcohol consumption. "Alcohol flushing" syndrome is attributable to elevated blood levels of acetaldehyde. However, even without the consumption of alcohol, aldehydes are produced endogenously as the major end products of lipid peroxidation.[7] Reactive oxygen species (ROS) are inevitably produced as byproducts of mitochondrial oxidative energy production.[8] Superoxide radicals are dismutated by superoxide dismutase (SOD) to produce hydrogen peroxides, which, in turn, are degraded into water and molecular oxygen by catalase, glutathione peroxidase, and peroxiredoxin. Hydroxyl radicals (OH•), which are the most potent ROS, are formed from hydrogen peroxide through the Fenton reaction. The OH• attack neighboring polyunsaturated fatty acids in the cell membrane, thereby triggering lipid peroxidation, which results in the generation of lipid hydroperoxides and α,β-unsaturated aldehydes, including 4-hydroxy-2-nonenal (4-HNE). These aldehydes are highly electrophilic and react with biomolecules such as proteins and nucleic acids to generate various adducts. By virtue of their high chemical stability, these lipid peroxidation products diffuse greater distances than their precursor ROS, so they can disseminate oxidative injury and amplify damage (Figure 1). Thus, it is now well accepted that much of the oxidative stress-associated damage can be attributed to aldehydes. Accumulation of aldehydes has been found in ischemic, hypertrophic, and failing hearts, as well as in oxidized low-density lipoprotein[9] atherosclerotic lesions, and the brains of patients with Alzheimer's disease.[10] Thus, aldehydes have been implicated in the pathogenesis of oxidative stress-associated diseases.

In addition to the pathogenic effect associated with oxidative stress, sublethal levels of aldehydes interact with signaling systems to upregulate the expression of genes to counteract the stressor challenge and to re-establish homeostasis[11–13] (Figure 2).

Sublethal Concentrations of 4-HNE Protect Cardiomyocytes Against Oxidative Injury via an NF-E2-Related Factor 2 (Nrf2)-Dependent Mechanism

Investigations into whether 4-HNE, one of the most abundant aldehydes produced by lipid peroxidation in vivo, induces stress response hormesis in cultured cardiomyocytes found that at higher concentrations (ie, ≥20 μmol/L) 4-HNE was cytotoxic but at lower concentrations it had no appreciable cytotoxicity (Figure 3).[14] Notably, pretreatment of cultured cardiomyocytes with a sublethal concentration of 4-HNE (5 μmol/L) for 14 h primed the cells to become resistant to subsequent exposure to cytotoxic concentrations of 4-HNE. Investigations into the mechanism underlying the cardioprotection mediated by 4-HNE revealed that, under normal (unstressed) conditions, Nrf2 is tethered to Keap1 in the cytoplasm. This complex directs Nrf2 polyubiquitination and degradation. During oxidative stress, Nrf2 is liberated from Keap1 and enters the nucleus, where it forms a heterodimer with the small Maf transcription factor, Nrf2, to induce the expression of genes for proteins that function as antioxidants and enzymes in phase II detoxification and glutathione biosynthesis.[15] 4-HNE induces the nuclear translocation of Nrf2 and enhances the expression of γ-glutamylcysteine ligase (GCL) and the core subunit of the Xc^- high-affinity cysteine transporter, thereby increasing intracellular GSH levels 1.45-fold. Cardiomyocytes treated with either Nrf2-specific short

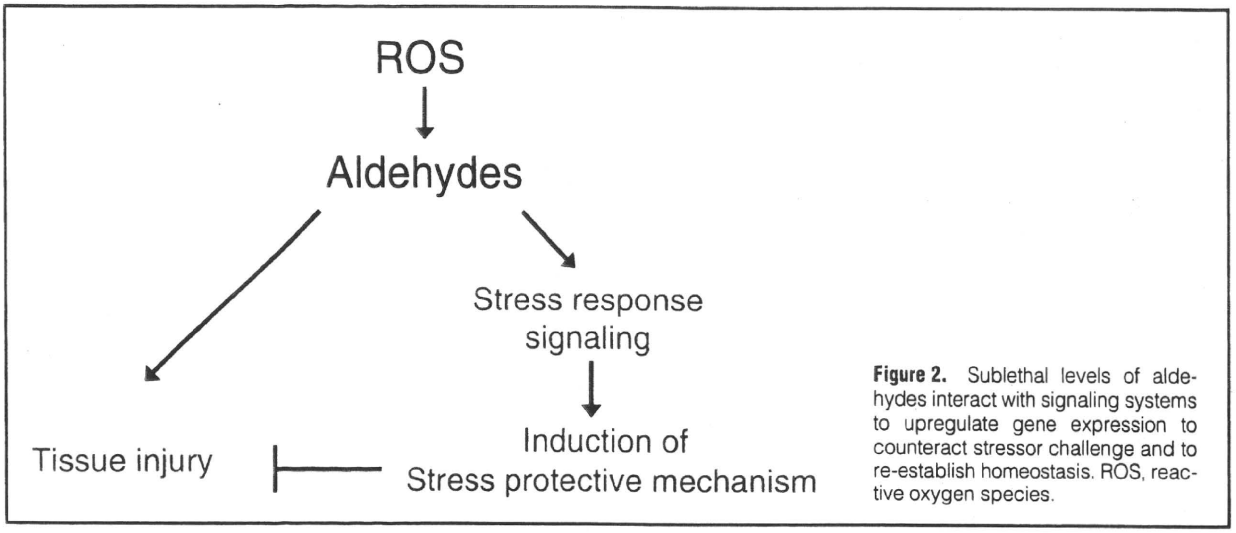

Figure 2. Sublethal levels of aldehydes interact with signaling systems to upregulate gene expression to counteract stressor challenge and to re-establish homeostasis. ROS, reactive oxygen species.

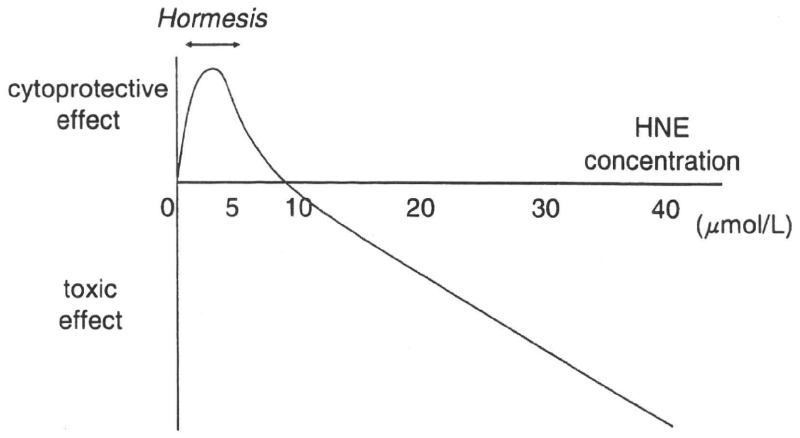

Figure 3. Hormetic effect of 4-hydroxy-2-nonenal (4-HNE) on cardiomyocytes.

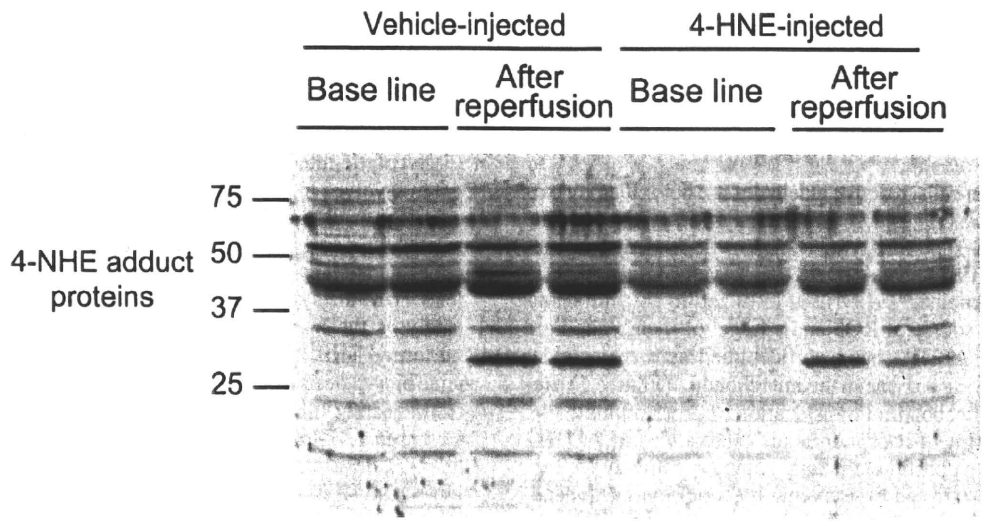

Figure 4. Pretreatment of mice with 4-hydroxy-2-nonenal (4-HNE) attenuated the increase in 4-HNE adduct proteins in response to ischemia–reperfusion injury.

interference (si) RNA or the GCL inhibitor L-buthionine sulfoximine were less tolerant to 4-HNE; moreover, the cardioprotective effect of 4-HNE pretreatment against subsequent ischemia–reperfusion injury was completely abolished in these cells. The mechanism by which 4-HNE induces the nuclear accumulation of Nrf2 remains to be determined. Specific cysteine residues (Cys273/Cys288) in the Keap1 protein are known to act as sensors for oxidative stress and modification of these residues leads to a conformational change in Keap1, with consequent release of Nrf2.[16] 4-HNE may induce a conformational change in Keap1 directly via adduct formation or indirectly by increasing the production of mitochondrial ROS.[17]

The cardioprotective effect of 4-HNE can be reproduced in vivo. When 4-HNE is injected via the retro-orbital vein, sufficient reactive 4-HNE reaches the heart. Cardiac Nrf2 is activated 60 min after systemic administration of 4-HNE, with subsequent Nrf-2-dependent upregulation of cardiac GSH and mRNA levels for antioxidant enzymes. In Langendorff-perfused mouse hearts, systemic administration of 4-HNE significantly improved the recovery of left ventricular function during ischemia–reperfusion. Consistent with these findings, levels of total lactate dehydrogenase released into the perfusate during reperfusion were significantly lower in 4-HNE-pretreated hearts than in control hearts. Ischemia–reperfusion significantly increased the levels of 4-HNE adduct proteins in the Langendorff-perfused hearts; notably, systemic administration of 4-HNE prior to ischemia significantly attenuated the increase in 4-HNE adduct proteins during reperfusion (**Figure 4**). This typeof cardioprotection was not seen in Nrf-2-knockout mice following the systemic administration of 4-HNE.[18]

Growing evidence indicates that a brief ischemic insult in 1 organ releases endogenous factors that protect other organs against a prolonged ischemic insult. This phenomenon is known as "remote ischemic preconditioning".[19] The exact nature of signal transduction from a remote tissue to the target organ remains to be elucidated. Although aldehydes conjugate easily with receptive nucleophiles (such as glutathione) in the circulating blood, these conjugates can stimulate stress resistance pathways in remote organs. These findings raise the possibility that aldehydes and/or their metabolites act as humoral mediators to mediate remote organ protection.

Aldehyde Dehydrogenase (ALDH) 2 Is a Major Aldehyde-Detoxifying Enzyme in the Mitochondria

In mammalian cells, reactive aldehydes are detoxified by oxidation to carboxylates, a reaction catalysed by ALDHs. The ALDHs are a superfamily of $NAD(P)^+$-dependent enzymes and, to date, 19 distinct ALDH genes have been identified in the human genome.[20] ALDH2 is localized to the mitochondria, a major source of ROS and a target of membrane lipid peroxidation. ALDH2 has been identified as a major aldehyde-detoxifying enzyme in the mitochondria (**Figure 1**). Recently, the mitochondrial translocation of protein kinase Cε and the subsequent phosphorylation (activation) of ALDH2 were shown to constitute the final common pathway for cardioprotection induced by ischemic preconditioning. Indeed, administration of a small-molecule activator of ALDH2 (ie, Alda-1) to rats before an ischemic event reduced infarct size by 60%.[21–23]

There is a polymorphism in the *ALDH2* gene specific to north-east Asian populations. The mutant allele *ALDH2*2* has a single point mutation of the active *ALDH2*1* gene, acting as a dominant negative gene. ALDH2 acts as a homo- or heterotetramer, and all tetramers that contain at least 1 ALDH2*2 subunit are inactive. People homozygous for the *ALDH2*2* allele (~8% of the Japanese population) do not have any ALDH2 activity, whereas activity in individuals heterozygous for the *ALDH2*2* allele (~40% of the Japanese population) is as low as one-sixteenth that in *ALDH2*1* (wild-type) homozygous individuals.[24] In addition to an association with alcohol flushing syndrome (commonly seen in people of Asian descent), the *ALDH2*2* allele is also associated with increased serum levels of lipid peroxides[25] and an increased risk of late-onset Alzheimer's disease.[26] However, favorable effects of the *ALDH2*2* allele have also been documented: the prevalence of proliferative retinopathy in Japanese patients with non-insulin-dependent diabetes mellitus is lower in the inactive ALDH2 compared with the active ALDH2 group,[27] although it remains to be clarified whether these correlations can be attributed to the hormetic effects of aldehydes in the retina.

Cardioprotection Can Be Achieved Within the Setting of Chronic Exposure to Aldehydes Throughout Life

To investigate whether a hormetic effect could be induced within the setting of the chronic exposure to aldehydes that persists throughout life, we created a loss-of-function model of Aldh2 by overexpressing *Aldh2*2*.[28] Consistent with the mitochondrial localization of the Aldh2*2 protein, levels of 4-HNE adduct proteins were increased in the mitochondrial, but not cytosolic, fraction of *Aldh2*2* transgenic (Tg) hearts. Interestingly, despite significant accumulation of 4-HNE adduct proteins in the mitochondrial matrices, left ventricular function in the *Aldh2*2* Tg mice was equivalent to that in their wild-type littermates until at least 2 years of age. Furthermore, the *Aldh2*2* Tg hearts exhibited greater tolerance to acute oxidative stress induced by ischemia–reperfusion than did wild-type hearts.

The expression of most major antioxidant enzymes, such as catalase, SOD, and GPx, was unaltered in *Aldh2*2* Tg hearts. Instead, there was upregulation of genes encoding enzymes involved in amino acid biosynthesis and transport in *Aldh2*2* Tg hearts. This included upregulation of genes encoding 3-phosphoglycerate dehydrogenase, phosphoserine aminotransferase, and phosphoserine phosphatase, all of which are involved in the 3-step conversion of 3-phosphoglycerate (a glycolytic intermetabolite) to serine, and upregulation of genes involved in various metabolic pathways that eventually converge on glutathione biosynthesis, such as serine hydroxymethyltransferase 1/2, which catalyses the conversion of serine and tetrahydrofolate (THF) to glycine and 5,10-methylene THF; methylenetetrahydrofolate dehydrogenase, which catalyses the interconversion of 5,10-methylene THF and 10-formyl THF; and cystathionase, which is involved in cysteine biosynthesis in the *trans*-sulfuration pathway (**Figure 5**). Consequently, intracellular concentrations of glutathione were increased 1.37-fold in *Aldh2*2* Tg compared with wild-type hearts. Consistent with this transcriptome analysis, metabolome analysis indicated that glucose uptake was upregulated in Tg hearts and that glucose biotransformation was shifted from glycolysis towards the pentose phosphate pathway to generate NADPH and amino acid biosynthesis,[29,30] which ultimately provide precursor amino acids for glutathione biosynthesis. Enhanced supply of NADPH via the pentose

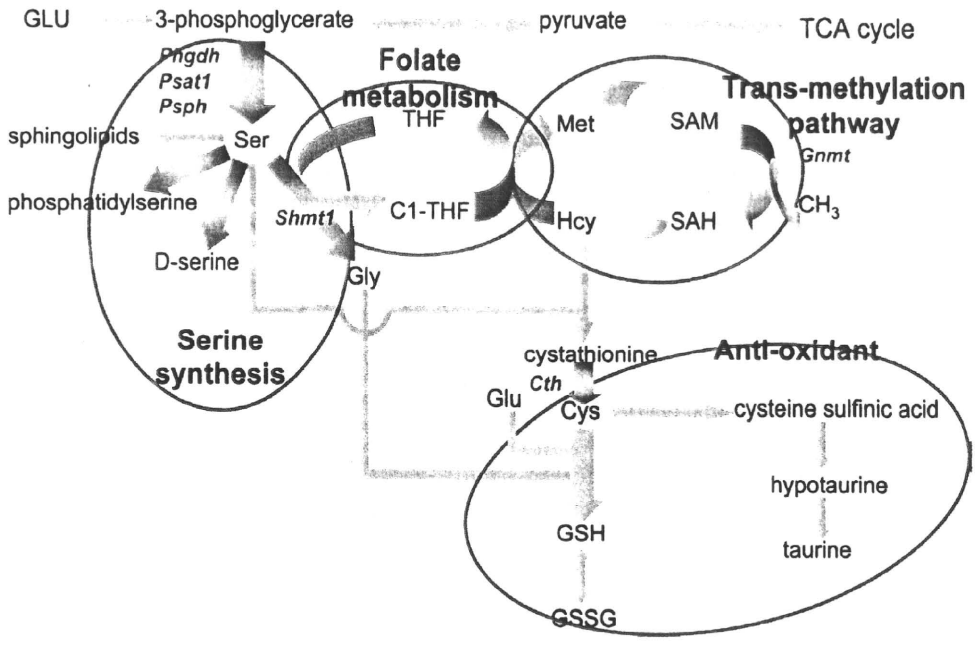

Figure 5. Activation of amino acid metabolism plays a key role in cardioprotection against chronic oxidative stress. Cys, cysteine; Gly, glycine; Glu, glutamate; GSH, glutathione; GSSG, oxidized glutathione; Gnmt, glycine N-methyltransferase; Hcy, homocysteine; Cth, cystathionase; Met, methionine; Phgdh, 3-phosphoglycerate dehydrogenase; Psat1, phosphoserine aminotransferase; Psph, phosphoserine phosphatase; SAH, S-adenosylhomocysteine; SAM, S-adenosylmethionine; Ser, serine; Shmt1, serine hydroxymethyltransferase 1; TCA, tricarboxylic acid; THF, tetrahydrofolate. Red arrows indicate enzymes that show significant increases in the Aldh2*2-Tg heart.

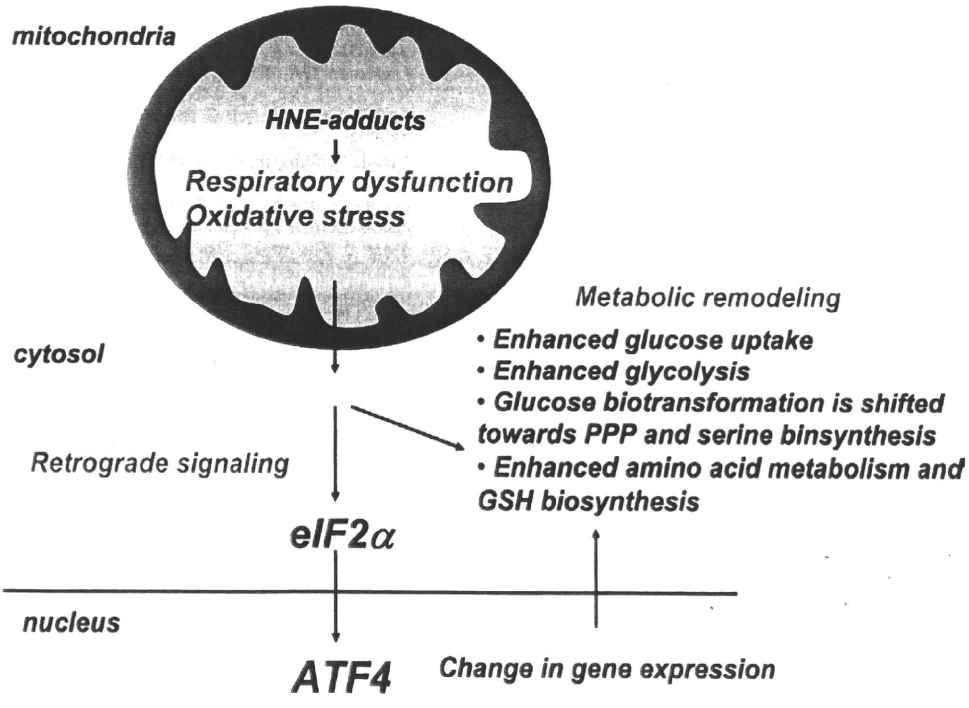

Figure 6. Mitochondrial oxidative stress activates retrograde signaling and confers enhanced tolerance to ischemia-reperfusion injury via metabolic remodeling. HNE, 4-hydroxy-2-nonenal; PPP, pentose phosphate pathway; GSH, glutathione; eIF2α, eukaryotic initiation factor 2α; ATF4, activating transcription factor 4.

phosphate pathway helps in the recycling of oxidized glutathione.

This work has extended the concept of cardioprotection by preconditioning. According to the current understanding of cardioprotection by preconditioning,[31] the mitochondria are the targets for protection from cell death. During sustained ischemia–reperfusion, the opening of the mitochondrial permeability transition pore (MPTP) induces mitochondrial swelling, depolarization, and ultimately cell death. Cardioprotection by preconditioning induced by brief non-lethal episodes of ischemia–reperfusion activates a variety of signaling cascades, all of which culminate in the inhibition of MPTP opening.[32] We have shown that mitochondrial retrograde signals (ie, signals originating from the mitochondria)[33] play a key role in cardioprotection (**Figure 6**). A shift towards the oxidative state in mitochondrial matrices sends a signal to the nucleus to change nuclear gene expression, enabling the cells to adapt to, and thus compensate for, mitochondrial oxidative stress.

The eukaryotic initiation factor (eIF) 2α–activating transcription factor 4 (Atf4) pathway[34–36] provides the key mitochondrial retrograde signals in response to mitochondrial aldehyde stress. Chronic mitochondrial aldehyde stress triggers phosphorylation of eIF2α and the combined transcriptional and translational activation of Atf4 upregulates the gene expression of enzymes involved in amino acid biosynthesis and transport that ultimately provide precursor amino acids for glutathione biosynthesis, thereby increasing intracellular glutathione levels. Indeed, heterozygous knockout of Atf4 blunted the increased expression of cardiac genes involved in amino acid metabolism and the increase in intracellular glutathione levels in *Aldh2*2* Tg hearts, thereby attenuating the oxidative stress-resistant phenotype.[37] These findings indicate that Atf4-dependent activation of amino acid metabolism and glutathione biosynthesis are causally involved in the oxidative stress-resistant phenotype observed in *Aldh2*2* Tg mice.

The study described above is limited by uncertainty as to whether the cardioprotection observed for *Aldh2*2* Tg hearts actually exists in individuals carrying the *ALDH2*2* allele. More generally, it would be of interest to determine whether a mitochondrial retrograde response transduced via the eIF2α–ATF4 pathway is involved in cardioprotection during human aging and in age-related diseases. Aging is accompanied by increased ROS production, with subsequently increased oxidative damage to mitochondrial DNA, proteins, and lipids. In addition, loss of cardioprotection in aged hearts is likely to be a consequence of an age-associated reduction in retrograde response signaling.[38] Notably, a paradoxical decline in relative levels of eIF2α Phosphorylation[39] and ATF4 expression have been demonstrated in aged rat tissues, including the heart, suggesting that the eIF2α–ATF4-mediated retrograde response to mitochondrial dysfunction operates less efficiently in the aged heart. How this retrograde regulation is affected by aging and age-related diseases is an important area for future research.

Conclusions

The cardiac stress response to aldehydes is accomplished by the activation of 2 basic leucine zipper transcription factors, namely Nrf2 and ATF4, at the posttranscriptional level.[40] These 2 transcription factors act in a coordinated manner to regulate glutathione biosynthesis and the glutathione redox cycle at different time points. Mimetic triggers of hormesis may be a promising approach to prevent the onset of oxidative stress-associated heart diseases and cardiac senescence itself without the risk of the overwhelming damage that is associated with the use of aldehydes themselves.

Acknowledgments

This work was supported by the Japan-China Medical Association and by a PRESTO (Metabolism and Cellular Function) grant from the Japanese Science and Technology Agency.

References

1. Minamino T, Komuro I. Vascular aging: Insights from studies on cellular senescence, stem cell aging, and progeroid syndromes. *Nat Clin Pract Cardiovasc Med* 2008; **5:** 637–648.
2. Epel ES, Blackburn EH, Lin J, Dhabhar FS, Adler NE, Morrow JD, et al. Accelerated telomere shortening in response to life stress. *Proc Natl Acad Sci USA* 2004; **101:** 17312–17315.
3. Colcombe SJ, Erickson KI, Raz N, Webb AG, Cohen NJ, McAuley E, et al. Aerobic fitness reduces brain tissue loss in aging humans. *J Gerontol A Biol Sci Med Sci* 2003; **58:** 176–180.
4. Ludlow AT, Zimmerman JB, Witkowski S, Hearn JW, Hatfield BD, Roth SM. Relationship between physical activity level, telomere length, and telomerase activity. *Med Sci Sports Exerc* 2008; **40:** 1764–1771.
5. Calabrese EJ, Baldwin LA, Holland CD. Hormesis: A highly generalizable and reproducible phenomenon with important implications for risk assessment. *Risk Anal* 1999; **19:** 261–281.
6. Gems D, Partridge L. Stress-response hormesis and aging: "That which does not kill us makes us stronger". *Cell Metab* 2008; **7:** 200–203.
7. Conklin D, Prough R, Bhatanagar A. Aldehyde metabolism in the cardiovascular system. *Mol Biosyst* 2007; **3:** 136–150.
8. Sano M. Mitochondrial protection and the reversal of left ventricular remodeling. *Circ J* 2009; **73:** 2017–2018.
9. Watson AD, Leitinger N, Navab M, Faull KF, Horkko S, Witztum JL, et al. Structural identification by mass spectrometry of oxidized phospholipids in minimally oxidized low density lipoprotein that induce monocyte/endothelial interactions and evidence for their presence in vivo. *J Biol Chem* 1997; **272:** 13597–13607.
10. Liu Q, Raina AK, Smith MA, Sayre LM, Perry G. Hydroxynonenal, toxic carbonyls, and Alzheimer disease. *Mol Aspects Med* 2003; **24:** 305–313.
11. Dickinson DA, Iles KE, Watanabe N, Iwamoto T, Zhang H, Krzywanski DM, et al. 4-hydroxynonenal induces glutamate cysteine ligase through JNK in HBE1 cells. *Free Radic Biol Med* 2002; **33:** 974.
12. Uchida K, Shiraishi M, Naito Y, Torii Y, Nakamura Y, Osawa T. Activation of stress signaling pathways by the end product of lipid peroxidation: 4-hydroxy-2-nonenal is a potential inducer of intracellular peroxide production. *J Biol Chem* 1999; **274:** 2234–2242.
13. Yang Y, Sharma R, Sharma A, Awasthi S, Awasthi YC. Lipid peroxidation and cell cycle signaling: 4-hydroxynonenal, a key molecule in stress mediated signaling. *Acta Biochim Pol* 2003; **50:** 319–336.
14. Zhang Y, Sano M, Shinmura K, Tamaki K, Katsumata Y, Matsuhashi T, et al. 4-Hydroxy-2-nonenal protects against cardiac ischemia-reperfusion injury via the Nrf2-dependent pathway. *J Moll Cell Cardiol* 2010 (in press).
15. Motohashi H, Yamamoto M. Nrf2-Keap1 defines a physiologically important stress response mechanism. *Trends Mol Med* 2004; **10:** 549–557.
16. Kobayashi A, Kang MI, Watai Y, Tong KI, Shibata T, Uchida K, et al. Oxidative and electrophilic stresses activate Nrf2 through inhibition of ubiquitination activity of Keap1. *Mol Cell Biol* 2006; **26:** 221–229.
17. Hill BG, Dranka BP, Zou L, Chatham JC, Darley-Usmar VM. Importance of the bioenergetic reserve capacity in response to cardiomyocyte stress induced by 4-hydroxynonenal. *Biochem J* 2009; **424:** 99–107.
18. Iida K, Itoh K, Kumagai Y, Oyasu R, Hattori K, Kawai K, et al. Nrf2 is essential for the chemopreventive efficacy of oltipraz against urinary bladder carcinogenesis. *Cancer Res* 2004; **64:** 6424–6431.
19. Kharbanda RK, Nielsen TT, Redington AN. Translation of remote ischaemic preconditioning into clinical practice. *Lancet* 2009; **374:** 1557–1565.
20. Vasiliou V, Pappa A, Estey T. Role of human aldehyde dehydrogenases in endobiotic and xenobiotic metabolism. *Drug Metab Rev*

2004; **36:** 279–299.
21. Churchill EN, Disatnik MH, Mochly-Rosen D. Time-dependent and ethanol-induced cardiac protection from ischemia mediated by mitochondrial translocation of varepsilonPKC and activation of aldehyde dehydrogenase 2. *J Mol Cell Cardiol* 2009; **46:** 278–284.
22. Chen CH, Budas GR, Churchill EN, Disatnik MH, Hurley TD, Mochly-Rosen D. Activation of aldehyde dehydrogenase-2 reduces ischemic damage to the heart. *Science* 2008; **321:** 1493–1495.
23. Perez-Miller S, Younus H, Vanam R, Chen CH, Mochly-Rosen D, Hurley TD. Alda-1 is an agonist and chemical chaperone for the common human aldehyde dehydrogenase 2 variant. *Nat Struct Mol Biol* **17:** 159–164.
24. Enomoto N, Takase S, Yasuhara M, Takada A. Acetaldehyde metabolism in different aldehyde dehydrogenase-2 genotypes. *Alcohol Clin Exp Res* 1991; **15:** 141–144.
25. Ohsawa I, Kamino K, Nagasaka K, Ando F, Niino N, Shimokata H, et al. Genetic deficiency of a mitochondrial aldehyde dehydrogenase increases serum lipid peroxides in community-dwelling females. *J Hum Genet* 2003; **48:** 404–409.
26. Kamino K, Nagasaka K, Imagawa M, Yamamoto H, Yoneda H, Ueki A, et al. Deficiency in mitochondrial aldehyde dehydrogenase increases the risk for late-onset Alzheimer's disease in the Japanese population. *Biochem Biophys Res Commun* 2000; **273:** 192–196.
27. Suzuki Y, Muramatsu T, Taniyama M, Atsumi Y, Kawaguchi R, Higuchi S, et al. Association of aldehyde dehydrogenase with inheritance of NIDDM. *Diabetologia* 1996; **39:** 1115–1118.
28. Endo J, Sano M, Katayama T, Hishiki T, Shinmura K, Morizane S, et al. Metabolic remodeling induced by mitochondrial aldehyde stress stimulates tolerance to oxidative stress in the heart. *Circ Res* 2009; **105:** 1118–1127.
29. Soga T, Heiger DN. Amino acid analysis by capillary electrophoresis electrospray ionization mass spectrometry. *Anal Chem* 2000; **72:** 1236–1241.
30. Soga T, Ueno Y, Naraoka H, Ohashi Y, Tomita M, Nishioka T. Simultaneous determination of anionic intermediates for *Bacillus subtilis* metabolic pathways by capillary electrophoresis electrospray ionization mass spectrometry. *Anal Chem* 2002; **74:** 2233–2239.
31. Heusch G, Boengler K, Schulz R. Cardioprotection: Nitric oxide, protein kinases, and mitochondria. *Circulation* 2008; **118:** 1915–1919.
32. Miura T, Miki T. GSK-3beta, a therapeutic target for cardiomyocyte protection. *Circ J* 2009; **73:** 1184–1192.
33. Liu Z, Butow RA. Mitochondrial retrograde signaling. *Annu Rev Genet* 2006; **40:** 159–185.
34. Wek RC, Jiang HY, Anthony TG. Coping with stress: eIF2 kinases and translational control. *Biochem Soc Trans* 2006; **34:** 7–11.
35. Kilberg MS, Pan YX, Chen H, Leung-Pineda V. Nutritional control of gene expression: How mammalian cells respond to amino acid limitation. *Annu Rev Nutr* 2005; **25:** 59–85.
36. Rutkowski DT, Kaufman RJ. All roads lead to ATF4. *Dev Cell* 2003; **4:** 442–444.
37. Tanaka T, Tsujimura T, Takeda K, Sugihara A, Maekawa A, Terada N, et al. Targeted disruption of ATF4 discloses its essential role in the formation of eye lens fibres. *Genes Cells* 1998; **3:** 801–810.
38. Boengler K, Schulz R, Heusch G. Loss of cardioprotection with ageing. *Cardiovasc Res* 2009; **83:** 247–261.
39. Hussain SG, Ramaiah KV. Reduced eIF2alpha phosphorylation and increased proapoptotic proteins in aging. *Biochem Biophys Res Commun* 2007; **355:** 365–370.
40. Sano M, Fukuda K. Activation of mitochondrial biogenesis by hormesis. *Circ Res* 2008; **103:** 1191–1193.

Zac1 Is an Essential Transcription Factor for Cardiac Morphogenesis

Shinsuke Yuasa, Takeshi Onizuka, Kenichiro Shimoji, Yohei Ohno, Toshimi Kageyama, Sung Han Yoon, Toru Egashira, Tomohisa Seki, Hisayuki Hashimoto, Takahiko Nishiyama, Ruri Kaneda, Mitsushige Murata, Fumiyuki Hattori, Shinji Makino, Motoaki Sano, Satoshi Ogawa, Owen W.J. Prall, Richard P. Harvey, Keiichi Fukuda

Rationale: The transcriptional networks guiding heart development remain poorly understood, despite the identification of several essential cardiac transcription factors.

Objective: To isolate novel cardiac transcription factors, we performed gene chip analysis and found that *Zac1*, a zinc finger–type transcription factor, was strongly expressed in the developing heart. This study was designed to investigate the molecular and functional role of Zac1 as a cardiac transcription factor.

Methods and Results: Zac1 was strongly expressed in the heart from cardiac crescent stages and in the looping heart showed a chamber-restricted pattern. Zac1 stimulated luciferase reporter constructs driven by *ANF*, *BNP*, or *αMHC* promoters. Strong functional synergy was seen between Zac1 and Nkx2-5 on the *ANF* promoter, which carries adjacent Zac1 and Nkx2-5 DNA-binding sites. Zac1 directly associated with the *ANF* promoter in vitro and in vivo, and Zac1 and Nkx2-5 physically associated through zinc fingers 5 and 6 in Zac1, and the homeodomain in Nkx2-5. *Zac1* is a maternally imprinted gene and is the first such gene found to be involved in heart development. Homozygous and paternally derived heterozygous mice carrying an interruption in the *Zac1* locus showed decreased levels of chamber and myofilament genes, increased apoptotic cells, partially penetrant lethality and morphological defects including atrial and ventricular septal defects, and thin ventricular walls.

Conclusions: Zac1 plays an essential role in the cardiac gene regulatory network. Our data provide a potential mechanistic link between Zac1 in cardiogenesis and congenital heart disease manifestations associated with genetic or epigenetic defects in an imprinted gene network. (*Circ Res*. 2010;106:1083-1091.)

Key Words: heart development ■ transcription factor ■ Zac1/Plagl1

The importance of transcription factors in development and cell differentiation has recently been underscored by the discovery that the introduction of 4 transcription factors into fibroblasts produces pluripotent stem cells.[1] Heart development is known to be regulated by a number of highly conserved transcription factors, although the mechanisms and logic of that regulation remain unclear. GATA4, myocyte enhancer factor (MEF)2C, serum response factor (SRF), Tbx5, and Nkx2-5 are expressed in the heart and play essential roles in its formation.[2–5] Furthermore, many of these transcription factors interact and act cooperatively and synergistically to direct cardiac developmental programs.[6] Despite their importance in cardiac development, however, none of the factors shows heart-specific expression, and it seems unlikely that a single factor determines cardiac cell fate.

We reported previously that transient treatment of differentiating embryonic stem cells with bone morphogenetic protein antagonists, efficiently induces cardiomyocyte differentiation.[7] Exploiting this system, we subsequently screened embryonic stem cell–derived cardiomyocytes for novel cardiac transcriptional factors using a gene chip analysis and found abundant cardiac expression of the zinc finger protein gene, *Zac1*. Zac1 was initially identified as an antiproliferative protein,[8] with subsequent studies implicating Zac1 in tumor suppression and organ development.[9,10] Furthermore, *Zac1* expression is regulated epigenetically during normal development. Imprinted genes are expressed from one allele according to their parent of origin, and this phenomenon is essential for mammalian embryogenesis. *Zac1* is a paternally expressed, imprinted gene.[10] Although imprinted genes are

Original received March 3, 2009; resubmission received December 1, 2009; revised resubmission received February 2, 2010; accepted February 5, 2010.

From the Department of Regenerative Medicine and Advanced Cardiac Therapeutics (S.Y., T.O., K.S., Y.O., T.K., S.H.Y., T.E., T.S., H.H., T.N., R.K., M.M., F.H., S.M., M.S., K.F.); Cardiology Division (S.Y., T.O., K.S., Y.O., T.K., S.H.Y., T.E., T.S., H.H., T.N., M.M., S.O.), Department of Internal Medicine; and Center for Integrated Medical Research (S.Y., S.M.), Keio University School of Medicine, Tokyo, Japan; Victor Chang Cardiac Research Institute (O.W.J.P., R.P.H.), Darlinghurst, New South Wales, Australia; and Faculties of Medicine and Science (R.P.H.), University of New South Wales, Kensington, Australia. Present address for O.W.J.P.: Walter and Eliza Hall Institute of Medical Research, Parkville, Victoria, Australia.

Correspondence to Keiichi Fukuda, MD, PhD, Professor and Chair, Department of Regenerative Medicine and Advanced Cardiac Therapeutics, Keio University School of Medicine, 35 Shinanomachi, Shinjuku, Tokyo 160-8582, Japan. E-mail kfukuda@sc.itc.keio.ac.jp

Circulation Research is available at http://circres.ahajournals.org

DOI: 10.1161/CIRCRESAHA.109.214130

Non-standard Abbreviations and Acronyms	
ANF	atrial natriuretic peptide
BNP	brain natriuretic peptide
ChIP	chromatin immunoprecipitation
E	embryonic day
EB	embryoid body
ES	embryonic stem
GST	glutathione *S*-transferase
LOT1	lost on transformation 1
MEF2C	myocyte enhancer factor 2C
MHC	myosin heavy chain
MLC	myosin light chain
P	postnatal day
PLAG	pleomorphic adenoma gene
SRF	serum response factor
ZRE	Zac1-response element

important for mammalian development, their roles in heart organogenesis are unknown.

In the present study, we investigated how Zac1 is involved in heart development. We show that Zac1 is an essential cardiac transcriptional factor, being highly expressed in mouse hearts from embryonic day (E)8.5 to adulthood in a chamber-restricted pattern. Zac1 was found to bind directly to the atrial natriuretic peptide gene (*ANF/Nppa*) promoter in vitro and in vivo, and to possess potent transcriptional activity. Nkx2-5 and Zac1 bound to adjacent sites within the *ANF* promoter, physically interacted, and synergistically activated cardiac gene expression. The *Zac1* promoter was activated by Nkx2-5 in vitro, whereas Nkx2-5–null mice showed decreased *Zac1* expression. Genetic inactivation of *Zac1* in mice (paternal-mutated heterozygote-descendent mice) induced defective embryonic heart development and reduced expression of chamber and myofilament genes. Our results indicate that Zac1 is an essential transcription factor for cardiac morphogenesis. Moreover, this is the first report that an imprinting gene mutation causes abnormal development of the heart.

Methods

Experimental procedures for in situ hybridization, animal study, immunostaining, Western blotting, plasmids, cell culture, electrophoretic mobility-shift assay, chromatin immunoprecipitation (ChIP) assay, glutathione *S*-transferase (GST) pull-down assay, RT-PCR analysis, and statistical analyses are provided in the expanded Methods section in the Online Data Supplement, available at http://circres.ahajournals.org.

Results

Zac1 Expression in the Embryonic Heart

We used gene chip analysis to search for novel cardiac transcription factors. Initially, we screened for genes upregulated in Noggin-treated differentiating embryonic stem (ES) cells that contained conserved transcription factor motifs and then confirmed the expression in the heart by whole-mount in situ hybridization. We also analyzed the transcriptional potency of each identified factor in vitro using the *ANF* promoter as target gene. The *ANF* promoter is a marker of the developing chamber myocardium, and is responsive to various signals, including those controlling cardiac growth, remodeling and pathological overload.[11] We screened for upregulated genes by comparing cardiomyocyte-rich differentiating ES cell–derived embryoid bodies (EBs) and nontreated EBs at day 6 of culture. Three hundred fifty-three genes were upregulated (>4-fold) in Noggin-treated EBs. Among them, 13 genes encoded a recognizable conserved transcription factor motif and had not yet been analyzed in the context of heart development. These were analyzed for cardiac expression, and 6 genes were analyzed for *ANF* promoter transactivation.

In situ hybridization of staged mouse embryos showed weak expression of *Zac1* in the cardiac crescent and other embryonic sites at E7.75 and stronger heart expression at E8.5, E9.0 and E9.5 (Figure 1A). Expression at E8.5 was enriched in chamber myocardium. Immunostaining revealed Zac1 protein expression in the heart at E8.5, E9.5, and E10.5, with a heart expression pattern similar to that of α-Actinin, but included more extensive expression in mesenchyme dorsal to the heart tube, corresponding to the second heart field (SHF) (Figure 1B). Zac1 protein expression was also enriched in chamber myocardium at E9.5 and E10.5, being lower in nonchamber myocardium of the atrioventricular canal (Figure 1B). In COS7 cells, overexpressed Zac1 was localized to the nucleus, as assessed by immunohistochemistry with an anti-Zac1 antibody (Figure 1C). Fractionation of COS7 cells transfected with increasing amounts of expression vector followed by SDS-PAGE and immunoblotting confirmed the specific accumulation of Zac1 in the nuclear (Figure 1D).

Zac1 Is a Potent Activator of *Nppa* Gene Expression

We used the gene promoters from *ANF*, brain natriuretic peptide (*BNP/Nppb*), and α-myosin heavy chain (*α-MHC/Myh6*) to evaluate the transactivational potency of Zac1 in COS7 cells in comparison to that of cardiac transcription factors MEF2C, GATA4, and SRF. Zac1 activated these promoters in a manner similar to the other factors (Figure 2A), in the case of *ANF* >250-fold. We also performed the luciferase assay using neonatal rat ventricular cardiomyocytes (Online Figure I). In these cells, Zac1 increased *ANF* and *BNP* promoter activities, as did the other transcription factors; however, relative transactivation was not as strong as in COS7 cells. The α-MHC promoter did not significantly respond to any of the factors, likely because cardiac transcription factors including Zac1 are strongly expressed in these cardiomyocytes and the effect of additional expression is weak or insignificant, depending on the promoter. Although Zac1 has been identified as a transcription factor and its binding sequence reported,[12] homologous sequences were not identified in the *ANF* promoter. To show that the Zac1-dependent *ANF* promoter activation was regulated in a DNA-binding–dependent manner, we constructed a series of *ANF* promoter mutants and mapped the *cis*-regulatory sequence that mediates the response to Zac1 to the region from

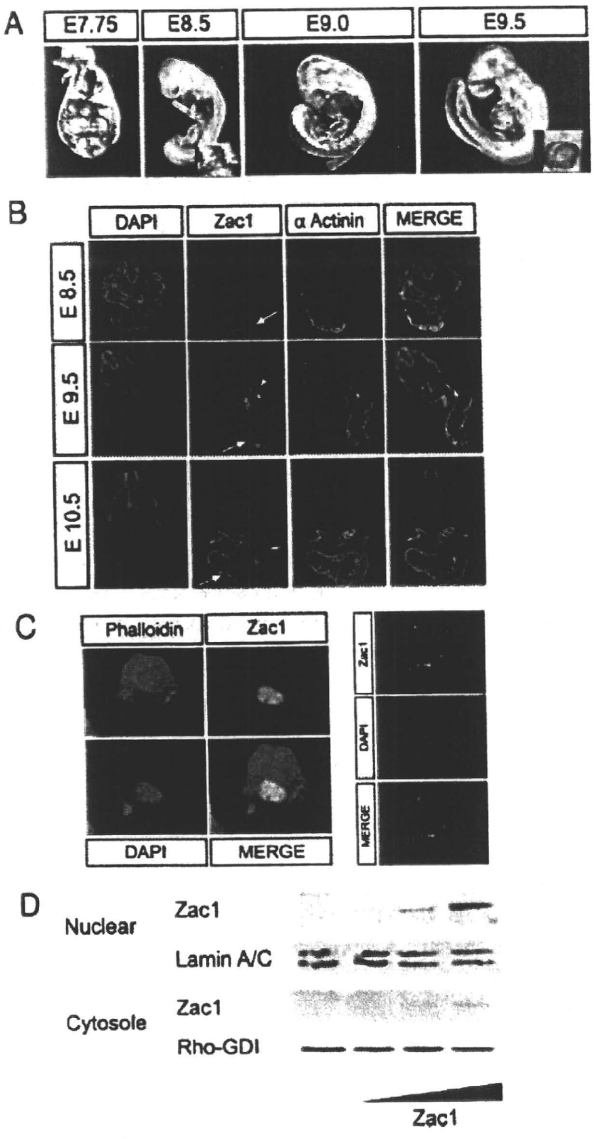

Figure 1. Expression of Zac1 in the murine embryonic heart. A, *Zac1* transcripts were detected in mouse embryos by whole-mount in situ hybridization. *Zac1* expression is weakly expressed in the cardiac crescent at E7.75 but detected throughout the heart at E8.5, E9.0, and E9.5. Frontal view of heart is shown in the **inset. B,** Immunostaining for the Zac1 protein in E8.5, E9.5, and E10.5 mouse embryos (transverse section). Zac1 protein is expressed in the heart enriched in chamber myocardium, whereas α-actinin is expressed throughout the heart and in the somites. Expression at E8.5 was enriched in chamber myocardium **(arrow)**. Zac1 expression included more extensive expression in mesenchyme dorsal to the heart tube, corresponding to the SHF **(arrowhead)**. Zac1 protein was also enriched in chamber myocardium **(arrow)** at E9.5 and E10.5, being lower in nonchamber myocardium of the atrioventricular canal **(short arrow). C,** Immunostaining of Zac1 protein in transfected COS7 cells, showing expression in the nucleus. **D,** Subcellular location of Zac1 protein in transfected COS cells, as detected by Western blotting. The nuclear accumulation of Zac1 is proportional to the DNA dosage used for transfection. Lamin A/C is a nuclear protein control, and Rho-GDI is cytosolic protein control.

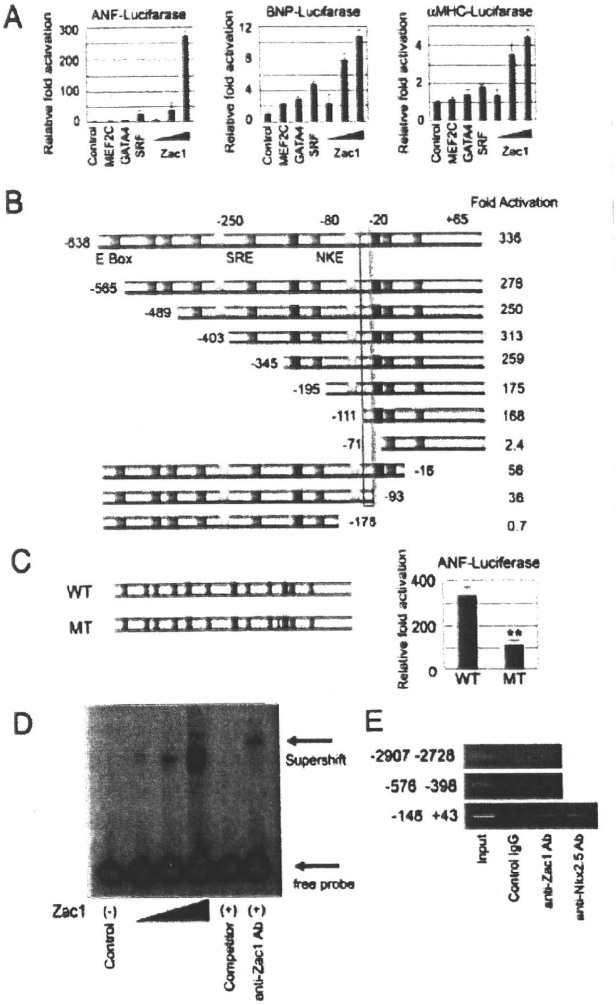

Figure 2. Zac1-transactivated ANF, BNP, and α-MHC genes. A, COS7 cells were cotransfected with a Zac1 expression plasmid and *ANF*, *BNP*, or *α-MHC*–luciferase reporter constructs. Values are expressed as the fold increase in luciferase activity compared to the empty expression plasmid (Control). **B,** COS7 cells were transfected with the Zac1 expression plasmid and the indicated *ANF* luciferase reporter constructs. Values are expressed as the fold increase in luciferase activity compared to the empty expression plasmid (Control). **Colored rectangles** indicate conserved transcription factor–binding site; **green box,** E box site; **blue box,** NKE; **yellow box,** SRF-binding element. **C,** COS7 cells were transfected with the Zac1 expression plasmid and the indicated *ANF* luciferase reporter constructs. The Zac1 response element is shown in blue (wild-type [WT]), and this element is mutated in the mutant (MT) promoter. **D,** Electrophoretic mobility-shift assay reveals the binding of Zac1 to radioactively labeled ZRE. Cold competitor interferes with the binding of Zac1 to the labeled ZRE. An antibody specific for Zac1 (anti-Zac1 Ab) supershifts the Zac1/ZRE complex. **E,** ChIP analysis reveals the binding of Zac1 and Nkx2-5 to the *ANF* promoter including the region −148 to +43 in vivo. PCR-amplified bands are apparent for the input DNA and anti-Zac1 antibody–precipitated DNA.

−111 to −93 (Figure 2B). The specific DNA sequence responsible for transactivation by Zac1 was further delineated by point mutagenesis. A Zac1-response element (ZRE) candidate sequence (GCCGCCG) within the *ANF* promoter was at least in part responsible for Zac1-dependent transactivation because mutation of this sequence to GTATATG attenuated responsiveness to Zac1 (Figure 2C). An electrophoretic mobility-shift assay was performed to determine whether Zac1 bound directly to this GCCGCCG sequence. The total amount of Zac1/DNA complex increased in proportion to the

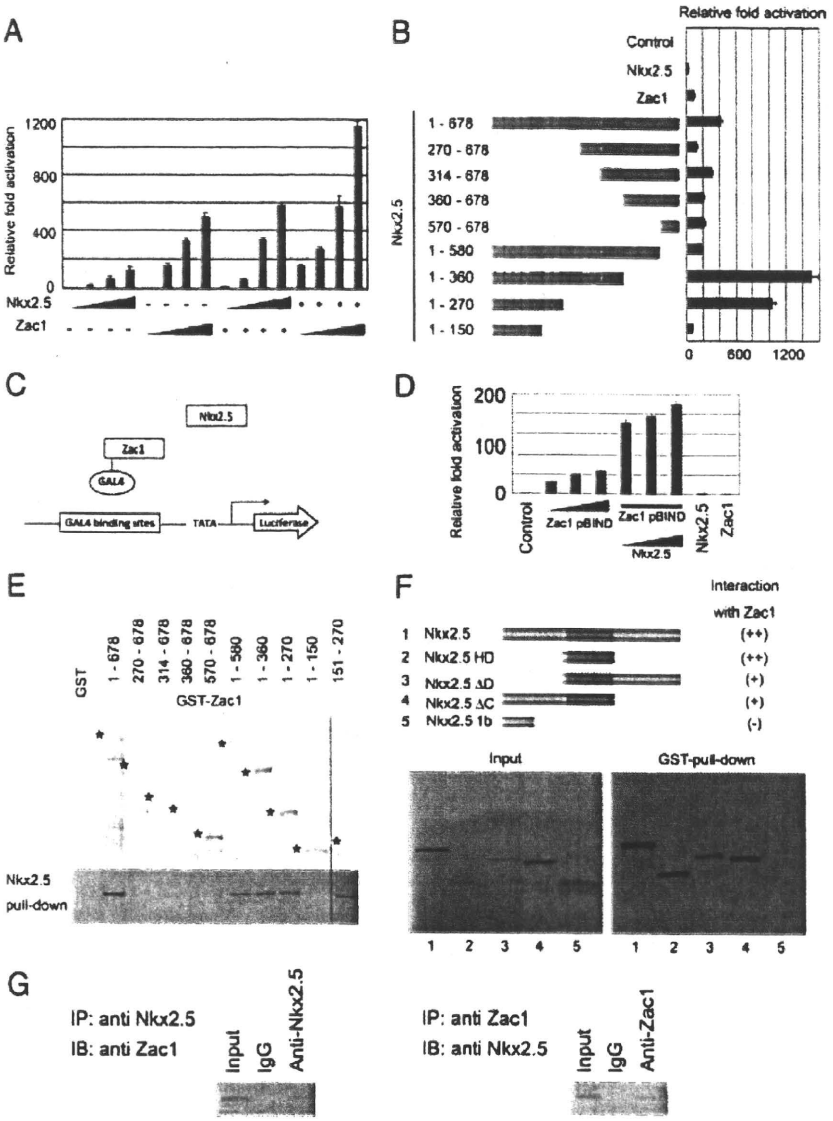

Figure 3. Zac1 and Nkx2-5 physically interact and synergistically activate *ANF* transcription. A, COS7 cells were transfected with ANF luciferase and expression vectors, encoding Nkx2-5 and Zac1. Both constructs synergistically activate *ANF* transcription (n=3). Nkx2-5 (10 to 300 ng); Zac1 (10 to 300 ng). **B,** Deletion mutants of *Zac1* were tested for their abilities to synergize with Nkx2-5 to activate *ANF* luciferase in COS7 cells. Values are expressed as fold increase in luciferase expression compared to the control. **Colored rectangles** indicate conserved protein motifs; **green box**, zinc finger motif; **blue and red boxes**, amelogenin motif; **brown box**, trypan PARP-like motif. **C,** Zac1 was fused with GAL4. A luciferase gene controlled by multiple GAL4-binding sites was used. Nkx2-5 cannot directly bind to GAL4 sites. **D,** Zac1-GAL4 increased the transactivation by DNA binding and Nkx2-5 increased this transactivation without direct DNA binding in presence of Zac1-GAL4. Wild-type Nkx2-5 and wild-type Zac1 alone did not show transactivation. **E,** GST-Zac1 deletion mutants were incubated with [^{35}S]methionine-labeled Nkx2-5 translated in vitro. The input Zac1 deletion mutant proteins are shown at **top.** Nkx2-5 proteins that bind to GST-Zac1 deletion mutants are shown at **bottom.** **F,** GST-Zac1 was incubated with [^{35}S]methionine-labeled Nkx2-5 deletion mutants translated in vitro. The input Nkx2-5 deletion mutant proteins are shown in the left panel. Nkx2-5 proteins that bind to GST-Zac1 deletion mutants are shown in the right panel. **G,** Coimmunoprecipitated proteins for Nkx2-5 or Zac1 were analyzed by immunoblotting using Zac1 or Nkx2-5 antibody. Nkx2-5 associated with Zac1 in neonatal heart extracts.

nuclear-localized Zac1 protein in COS7 cells at increasing DNA dosage. Furthermore, this complex was extinguished by the addition of cold competitor and was supershifted by the anti-Zac1 antibody (Figure 2D). To confirm that Zac1 binds to the *ANF* promoter in vivo, we used a ChIP assay. Cross-linked chromatin obtained from neonatal rat hearts was immunoprecipitated with the anti-Zac1 antibody. The precipitated chromatin DNA was then purified, and PCR analysis for enrichment of the target sequences revealed that Zac1 bound directly to the *ANF* promoter in vivo (Figure 2E). ChIP assay also showed that Nkx2-5 bound to same promoter region which includes an Nkx2-5–binding region (NKE). Zac1 did not bind to distant promoter regions which do not include a ZRE.

Zac1 Activates *ANF* Gene Expression Synergistically With Nkx2-5

The Zac1 DNA-binding site within the *ANF* promoter is adjacent to the reported binding site for Nkx2-5.[13] Therefore, we used the *ANF* promoter to ascertain whether Zac1 acts synergistically with Nkx2-5 to activate transcription. Vectors for these transcription factors were cotransfected at different DNA dosages into COS7 cells (Figure 3A). Zac1 activated the *ANF* promoter >1100-fold in a dose-dependent manner and this required the presence of Nkx2-5. Moreover, maximum activation by Nkx2-5 (>600 fold) required Zac1. To identify the protein domain of Zac1 that is involved in this synergistic activity with Nkx2-5, we cotransfected several mutated forms of Zac1 and Nkx2-5 into COS7 cells and measured the transcriptional activity of the *ANF* promoter (Figure 3B). Deletion of the 6 zinc finger domains in Zac1 (green domains in Figure 3B) reduced its ability to stimulate transcription. Notably, carboxyl-terminal deletion mutants 1 to 360 and 1 to 270, which potentially lack C-terminal repression domains, showed strong synergistic activities with Nkx2-5 (1000- to 1400-fold), which in turn was reduced by deletion of the zinc finger 5 and 6 domains (Figure 3B). Therefore, our data implicate zinc finger domains 5 and 6 of Zac1 in the functional interaction with Nkx2-5. To clarify the requirement of DNA binding for the interaction between